Cosmology and Cluster Astrophysics with Cross-Correlations of HSC WL and Planck tSZ

Kavli IPMU Astro Lunch Seminar
November 26, 2019

Ken Osato
Institut d'Astrophysique de Paris

ArXiv: 1910.07526

Collaborators:
Masato Shirasaki (NAOJ), Hironao Miyatake (Nagoya),
Daisuke Nagai (Yale), Naoki Yoshida (UTokyo, Kavli IPMU),
Masamune Oguri (UTokyo), and Ryuichi Takahashi (Hirosaki)
HSC WL WG

Contents

1. **Introduction**

2. **Method: model and covariance**

3. **Measurements and analysis of tSZ-WL cross-correlation with HSC and *Planck***

4. **Future prospects and summary**

Cluster Cosmology and Astrophysics

Planck col. (2016)

Cluster cosmology

The abundance of clusters and mass profi le of clusters are powerful probes into large-scale structures. However, there is a tension on cosmological parameters, e.g., **sigma8 tension**.

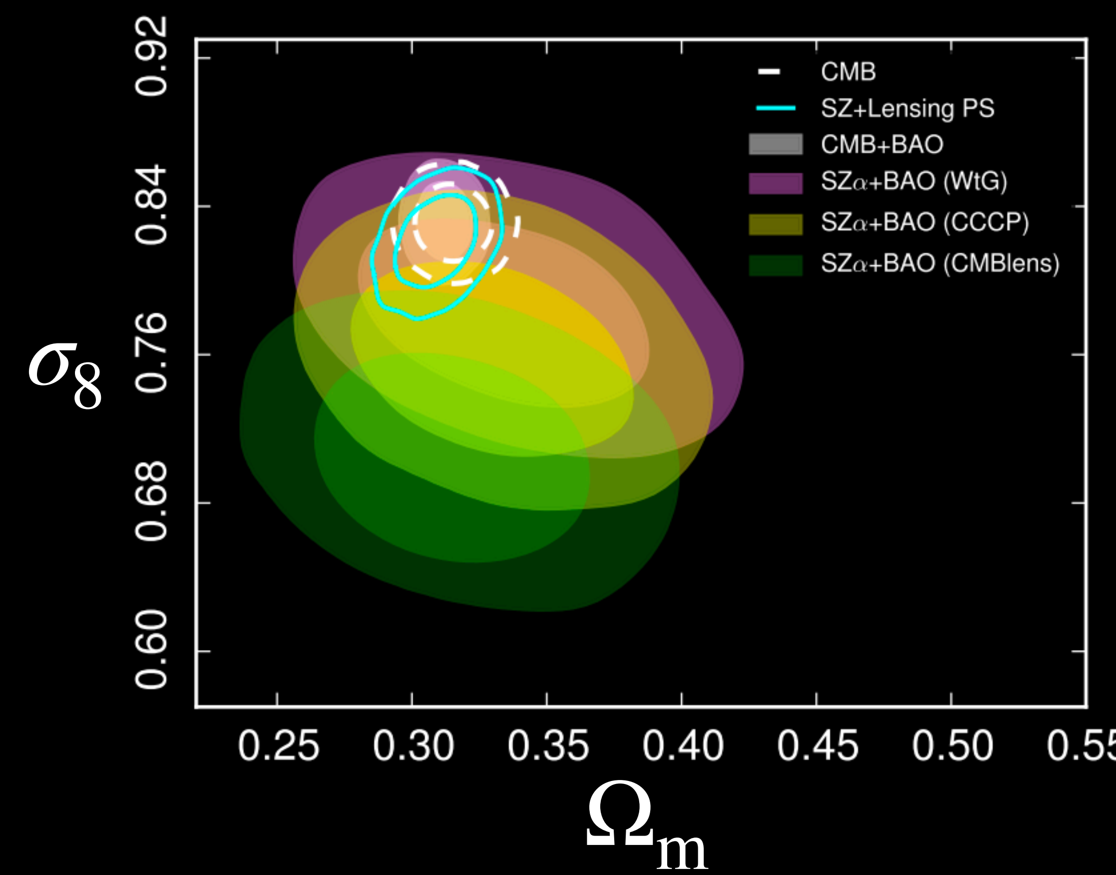

Non-thermal pressure

Some physical processes other than thermal pressure, e.g., **turbulence**, can also support the self-gravity of galaxy clusters. The mass under hydrostatic equilibrium (HSE) is parameterized as

$$\frac{M_{\rm HSE}}{M_{\rm true}} = 1 - b$$

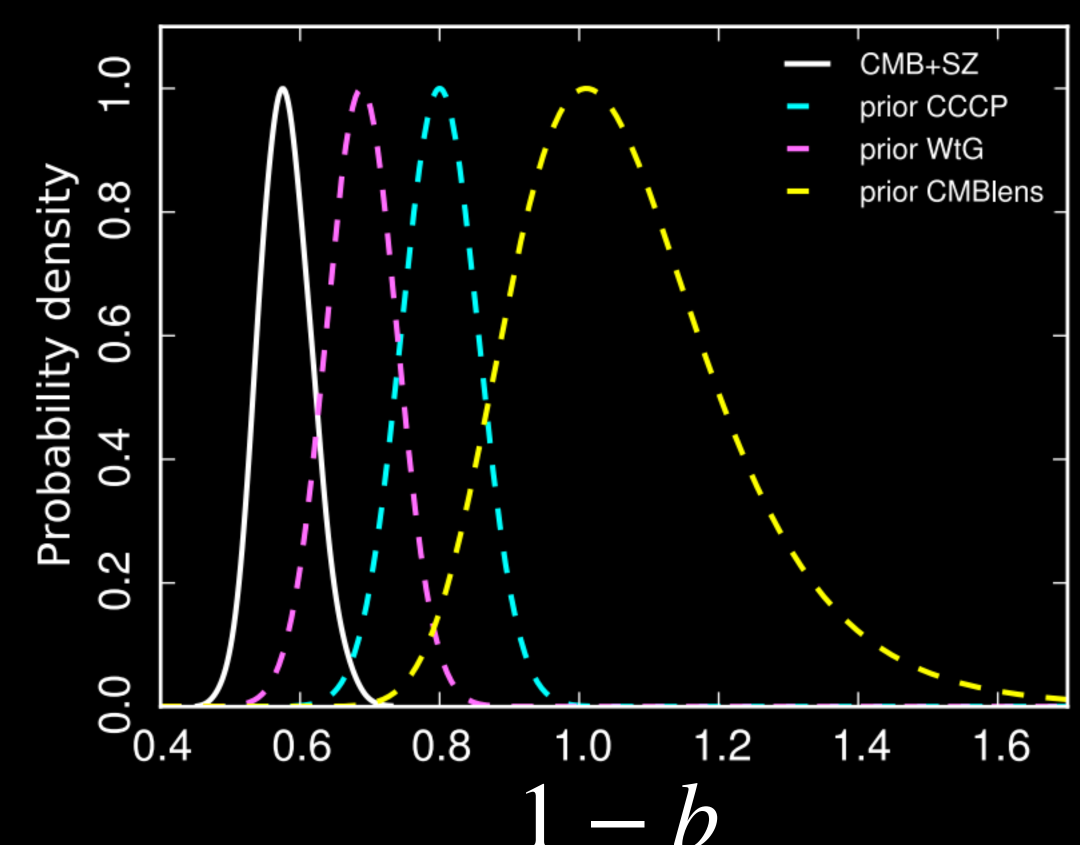

Weak Gravitational Lensing

The ***large-scale structures*** induce weak gravitational lensing effect.
We can probe into the matter distribution in an **unbiased** way.

The images of galaxies are distorted due to the foreground gravitational field, and the distortion can be detected by statistically analyzing many images.

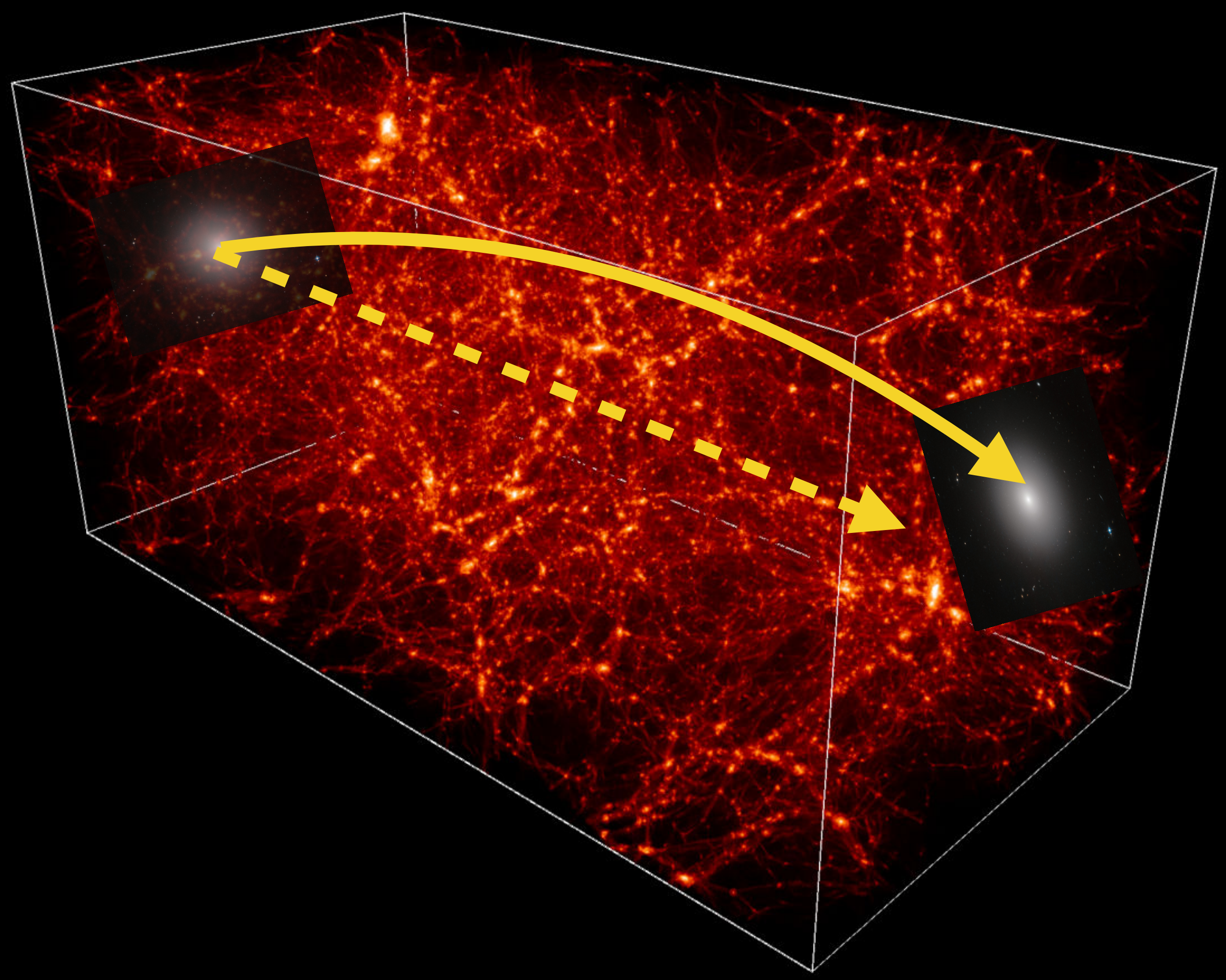

Convergence field:

$$\kappa(\theta) = \frac{3}{2}\left(\frac{H_0}{c}\right)^2 \Omega_{\rm m} \times \int d\chi\, f(\chi_s, \chi)\delta(D_A(\chi)\theta, \chi)$$

lensing kernel **density**

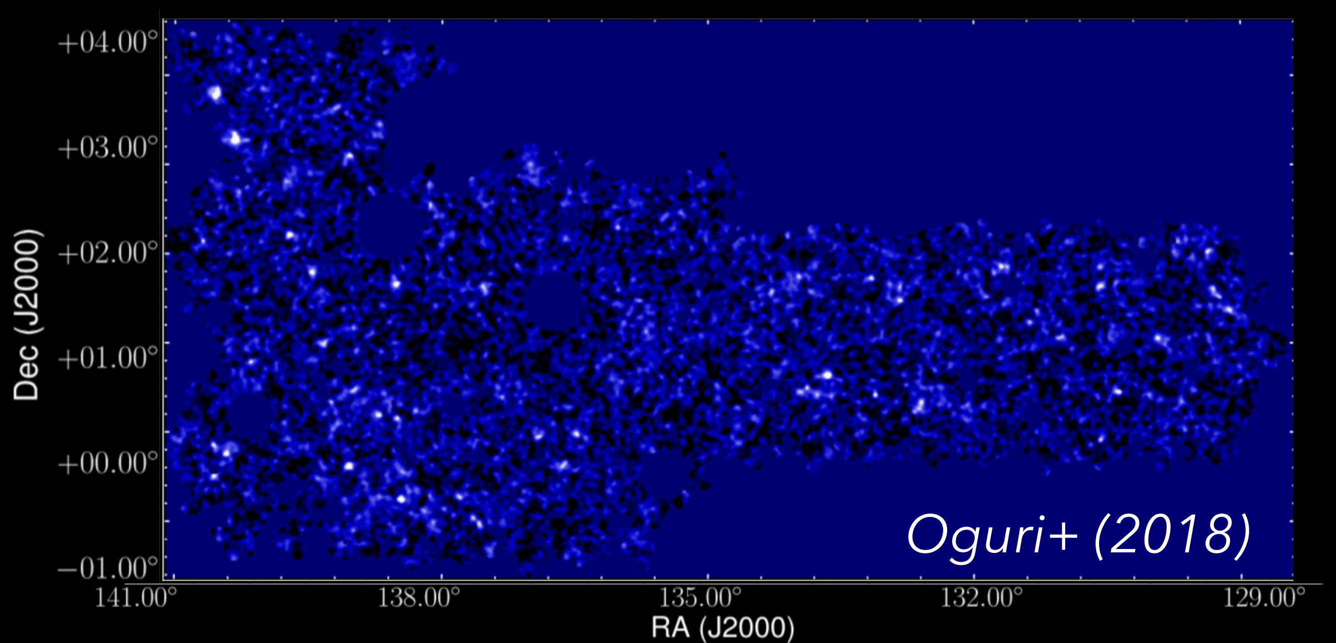

2D mass map from HSC

The Sunyaev-Zel'dovich Effect

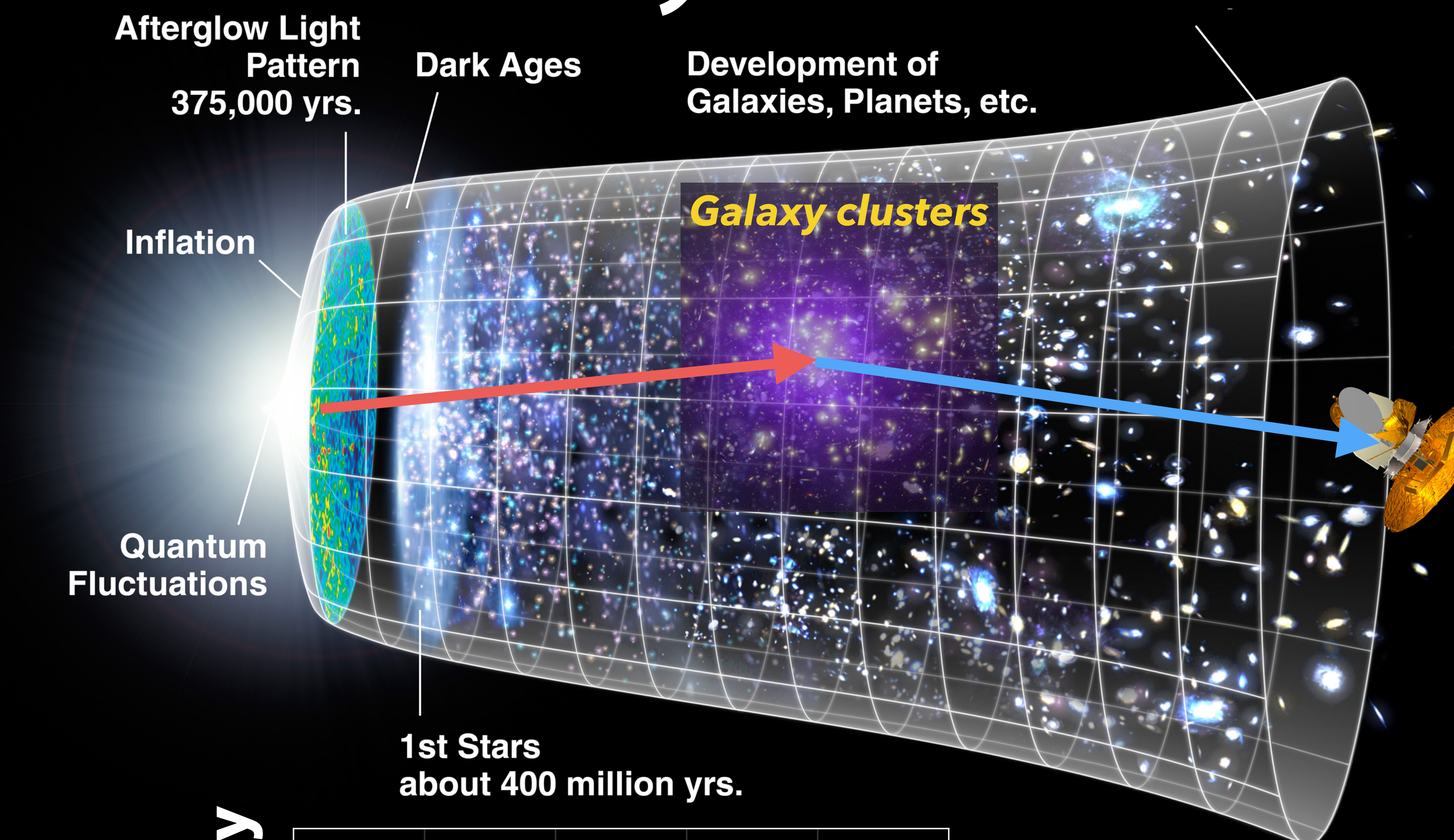

all-sky Compton-y map by Planck

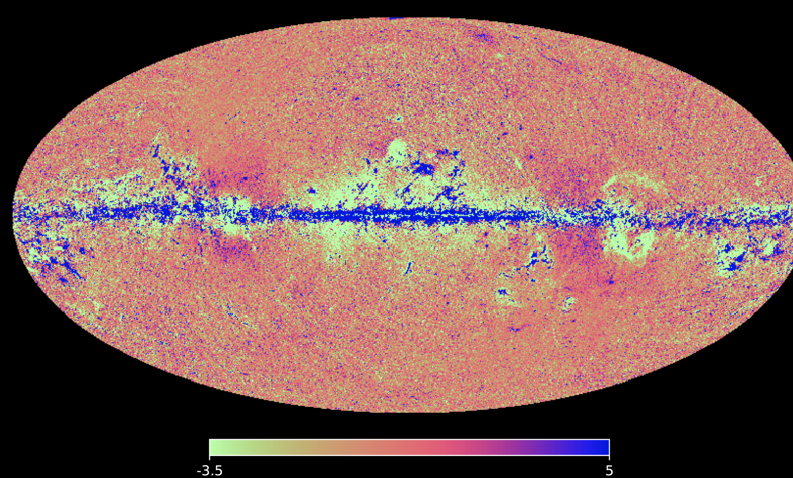

Planck col. (2016)

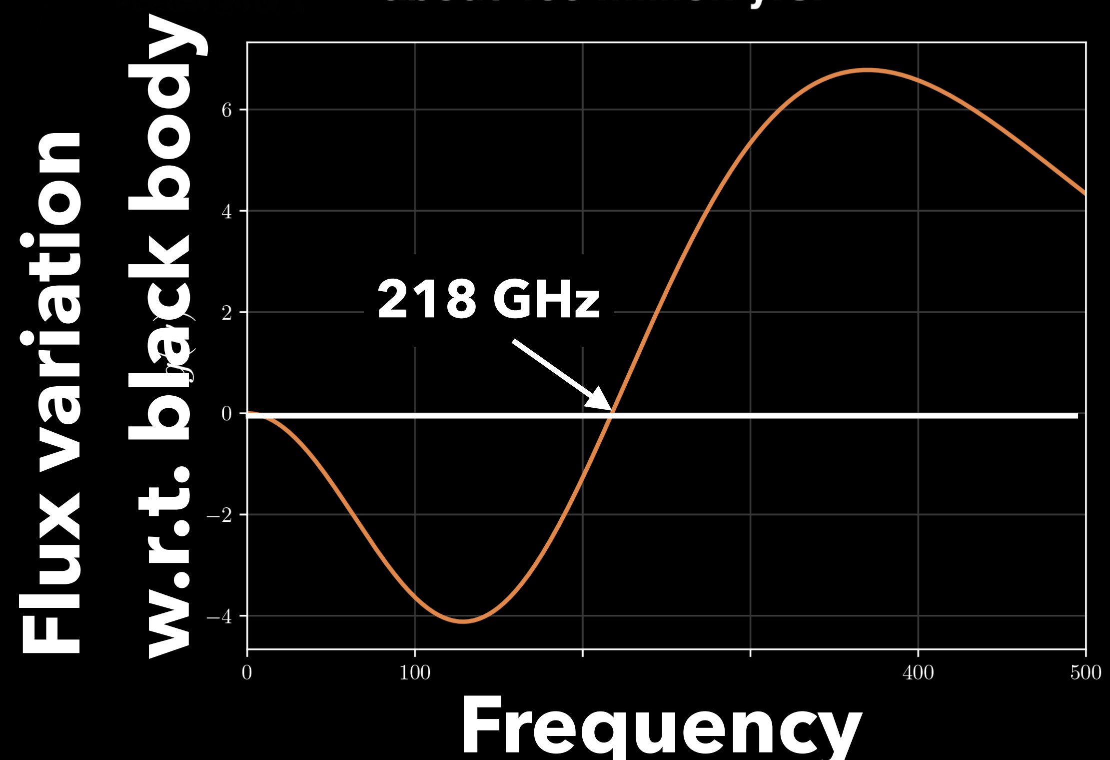

$$\frac{\Delta T}{T} = y\left(x\frac{e^x+1}{e^x-1}-4\right),\ x=\frac{h\nu}{kT}$$

Compton-y $$y = \frac{\sigma_{\mathrm{T}} k_{\mathrm{B}}}{m_e c^2}\int P_e\, dl$$

Sunyaev and Zel'dovich (1972, 1980)

Cosmology with WL and tSZ

HSC cosmic shear analysis

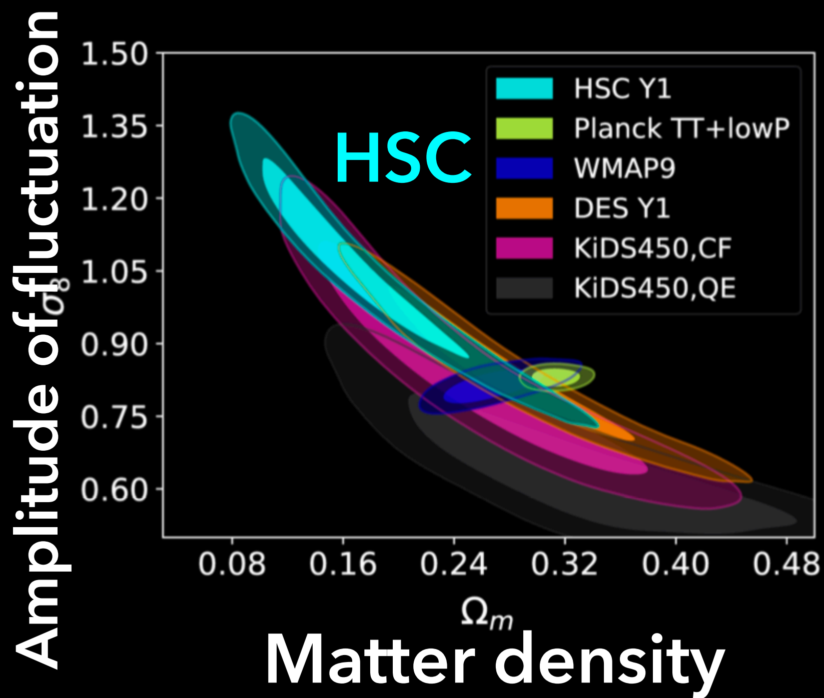

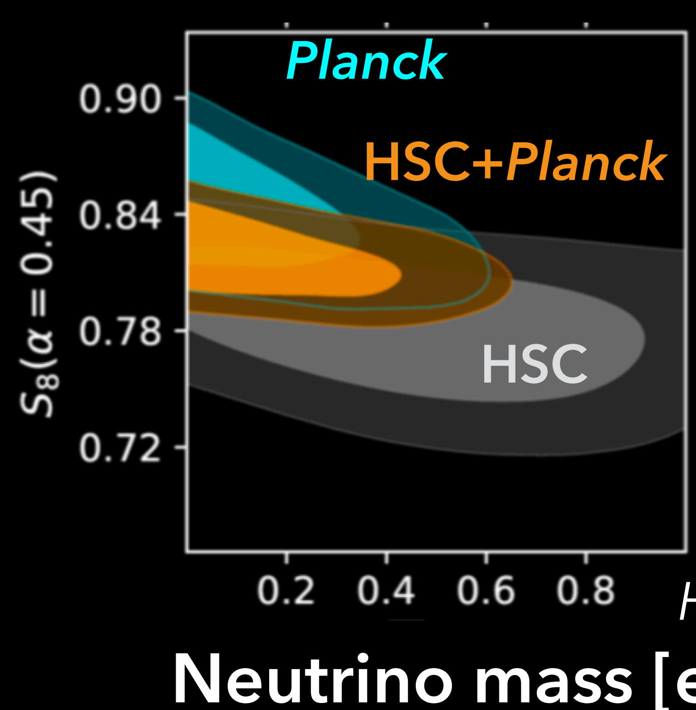

Hikage+ (2018)

tSZ auto-power spectrum analysis

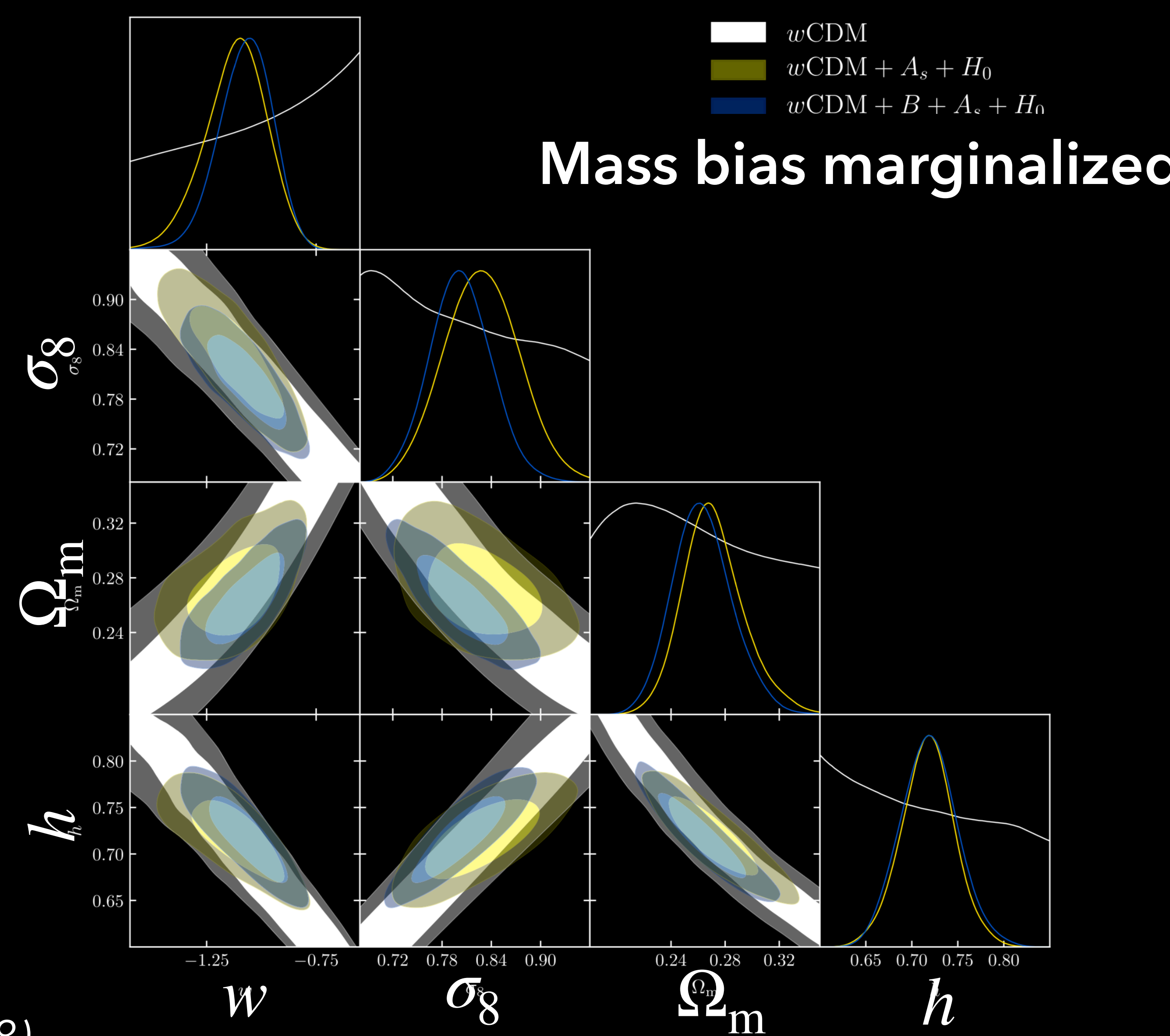

Bolliet+ (2018)

Auto 2pt Correlations

WL

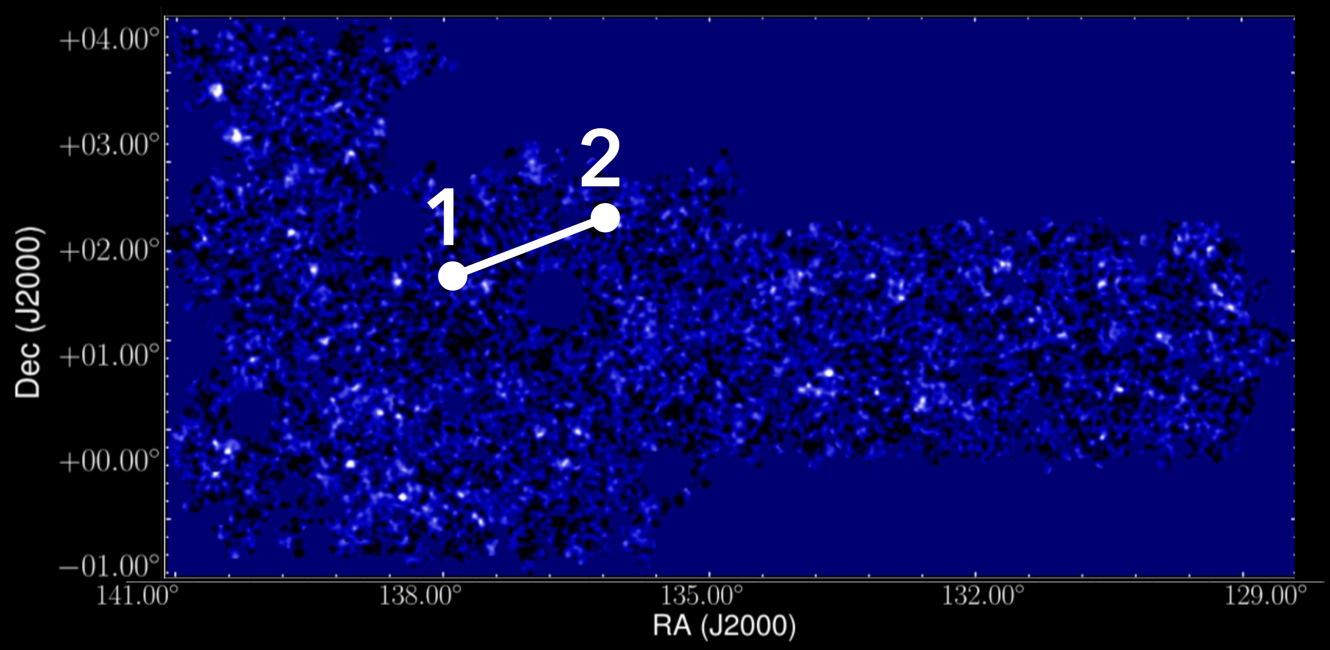

Power spectrum / 2pt correlation

Cosmology

tSZ

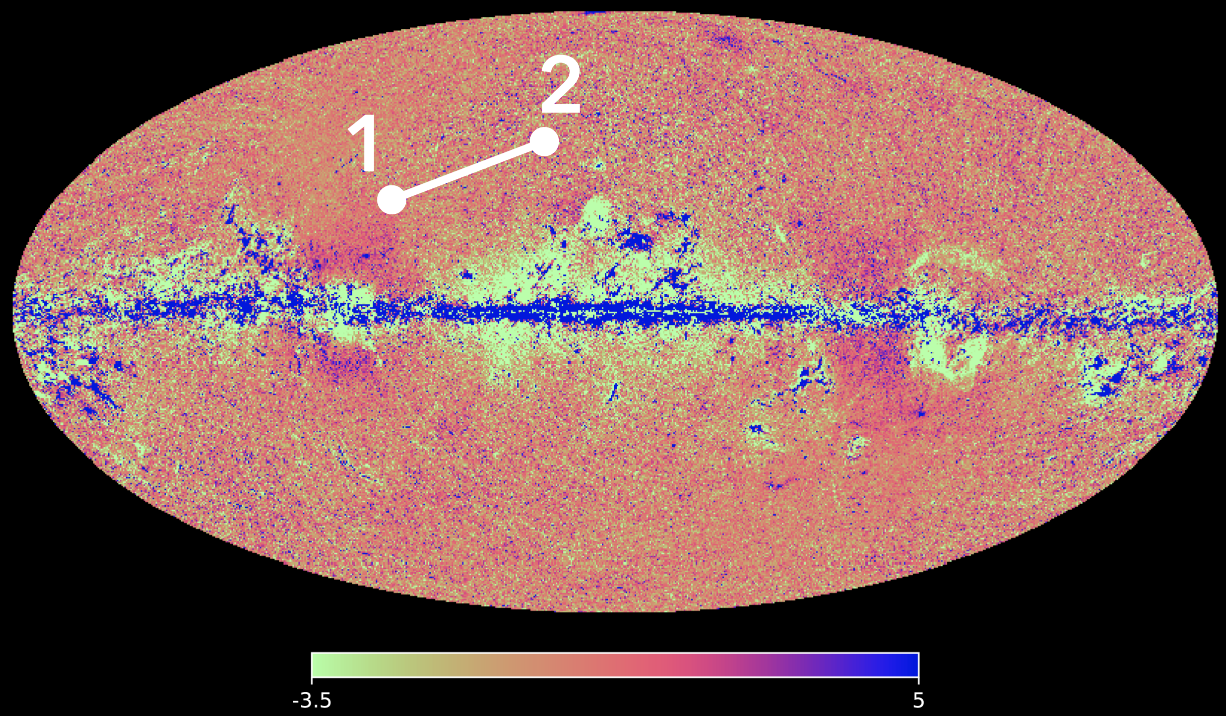

Cosmology

Power spectrum / 2pt correlation

Auto 2pt Correlations

WL

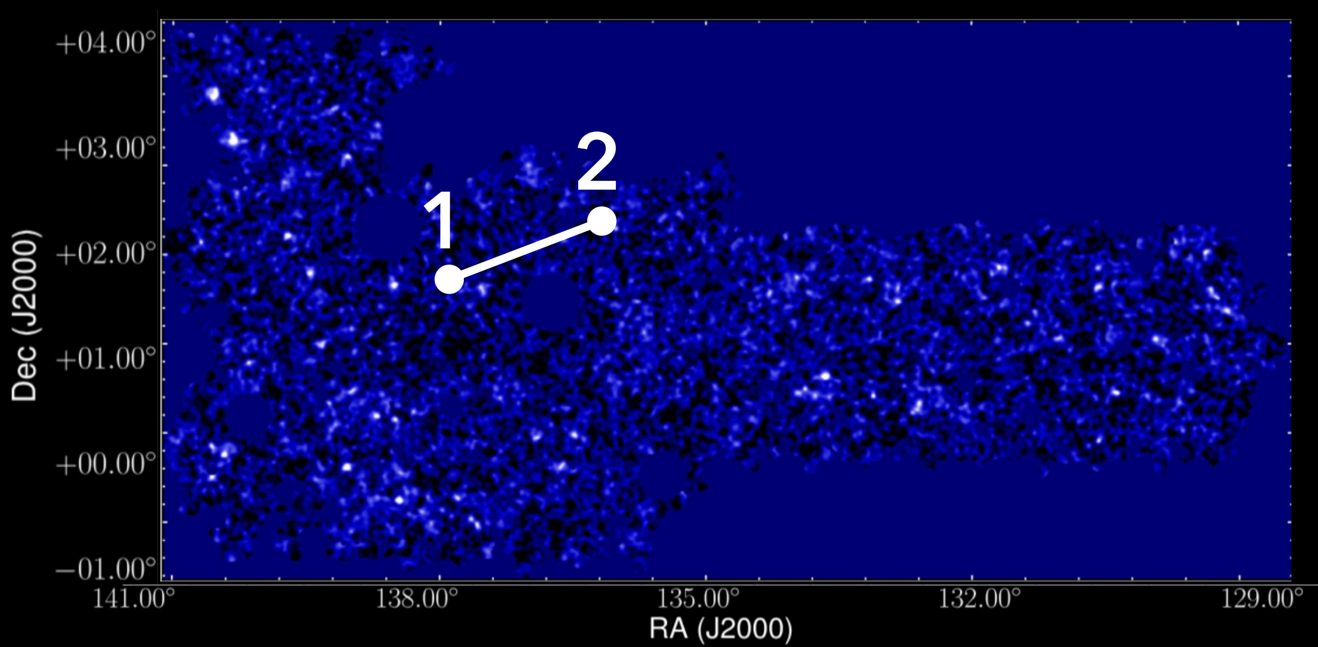

tSZ

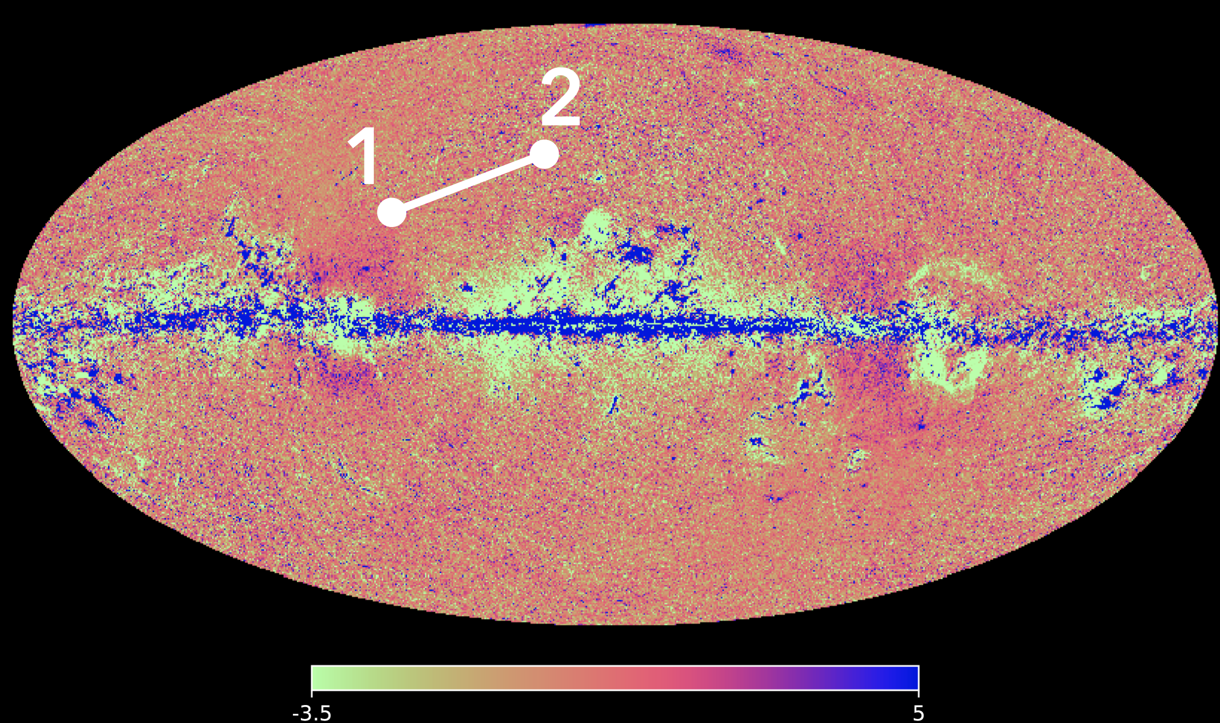

Power spectrum / 2pt correlation

Cosmology

Joint Analysis?

Cosmology

Power spectrum / 2pt correlation

Cross 2pt Correlations

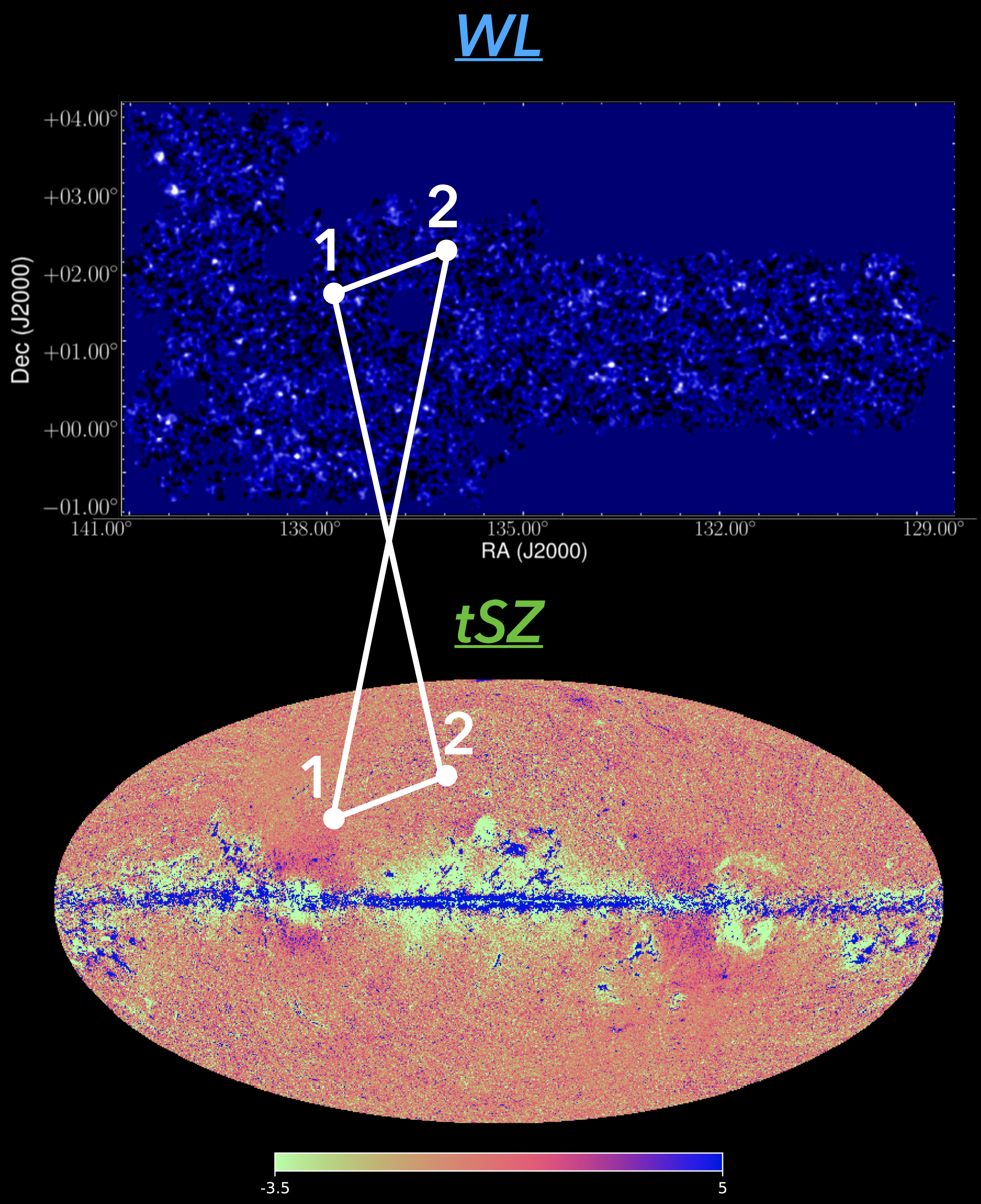

Cross-correlations!

✦Especially in the case of cross-correlation between ***high S/N*** and *low S/N* observables, the cross-correlation becomes more powerful!

X = **WL**, galaxies, CMB temp.

Y = **tSZ,** CMB pol., GW source

$$\frac{(S/N)^2_{\rm XY}}{(S/N)^2_{\rm YY}} \gg 1$$

Cross-Correlations of tSZ-WL

✦**Measurements of tSZ-WL cross-correlations**

The cross-correlation between thermal SZ effect and weak lensing has been measured from *Planck* and CFHTLenS (RCSLenS) data.

cf. van Waerbeke+ 2014, Hojjati+ 2016

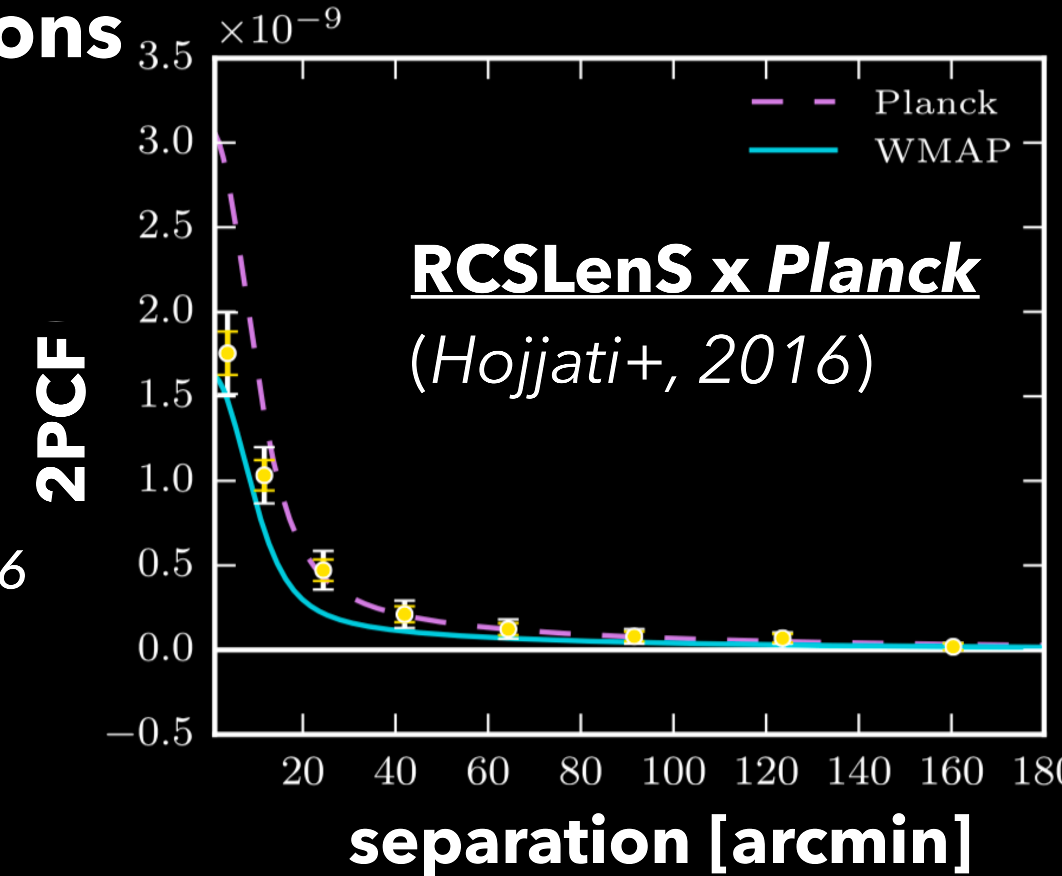

➡We can constrain both of cosmological parameters (**cosmology**) and hydrostatic mass bias (**astrophysics**) with tSZ auto-power spectrum and tSZ-WL cross-correlations.

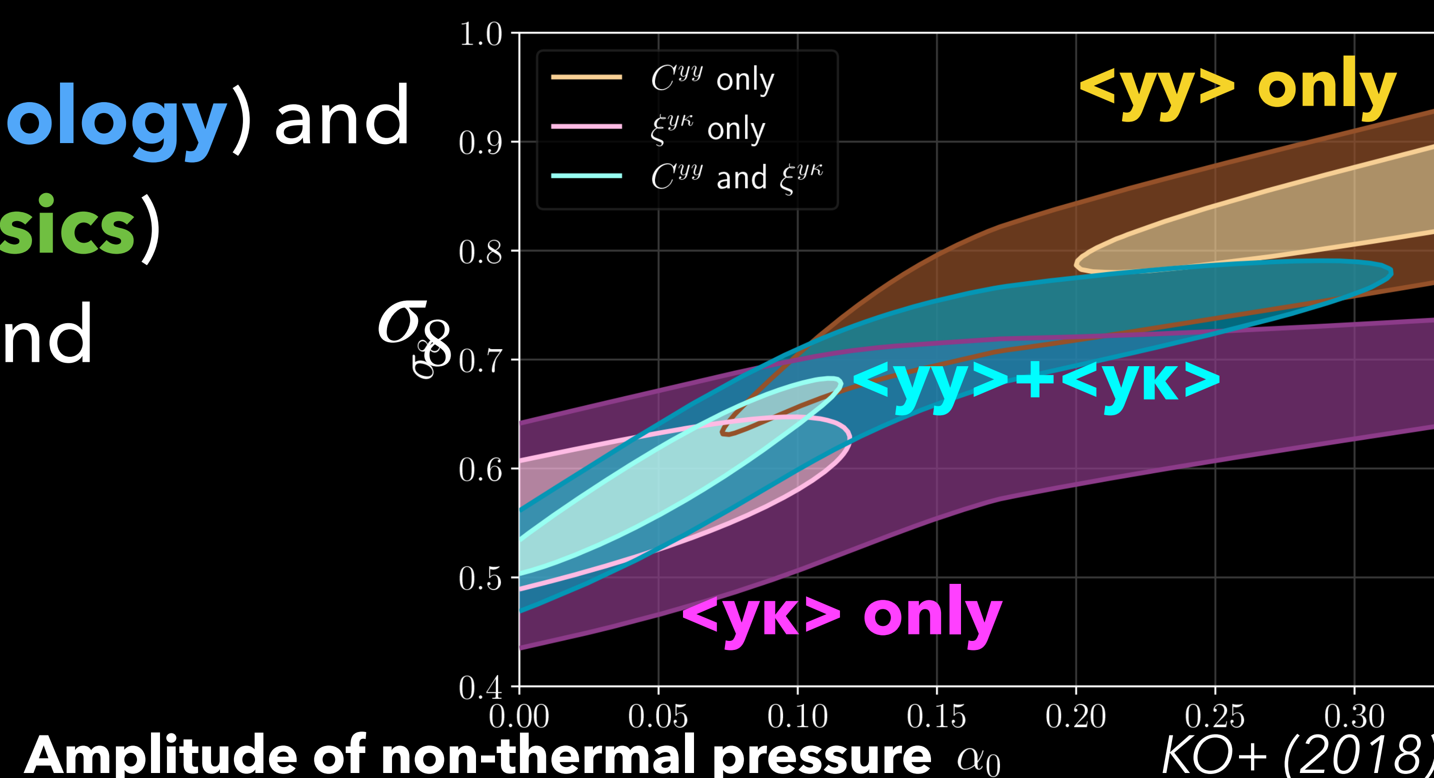

KO+ (2018)

Cross-Correlations of tSZ-WL

✦**Measurements of tSZ-WL cross-correlations**

The cross-correlation between thermal SZ effect and weak lensing has been measured from *Planck* and

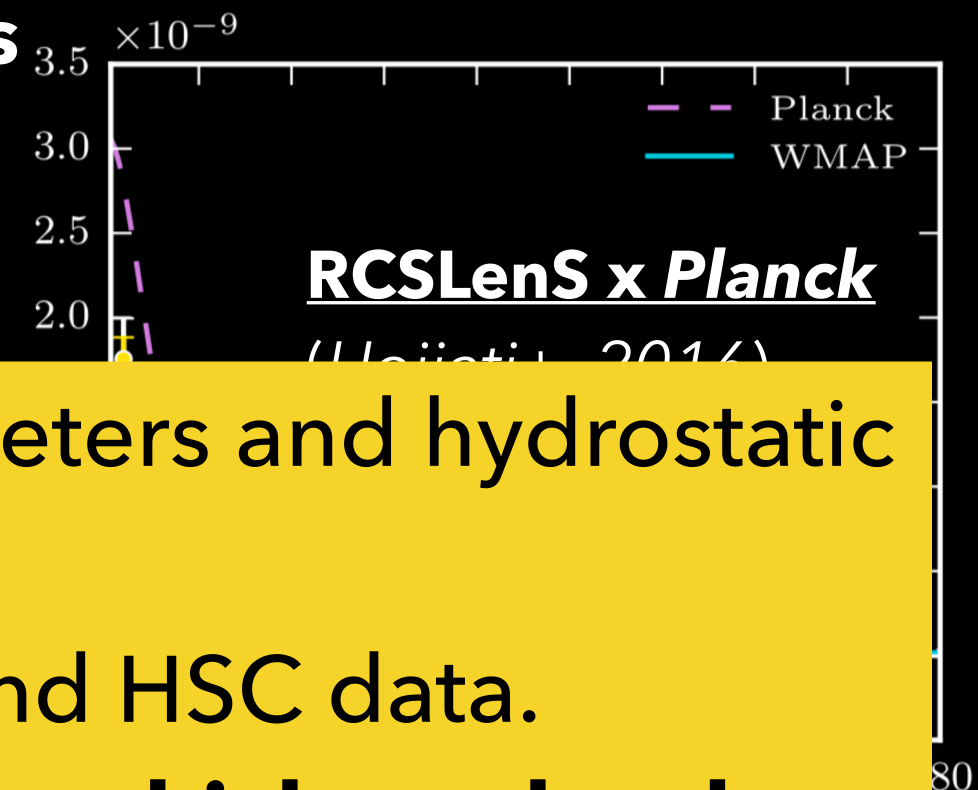

Goal: Constraining cosmological parameters and hydrostatic mass bias parameter with tSZ auto- and tSZ-WL cross-correlations from *Planck* and HSC data.

The low-mass or high-redshift clusters, which are hard to be observed through X-ray or SZ, contribute to the signal.

cosmological parameters (**cosmology**) and hydrostatic mass bias (**astrophysics**) with tSZ auto-power spectrum and tSZ-WL cross-correlations.

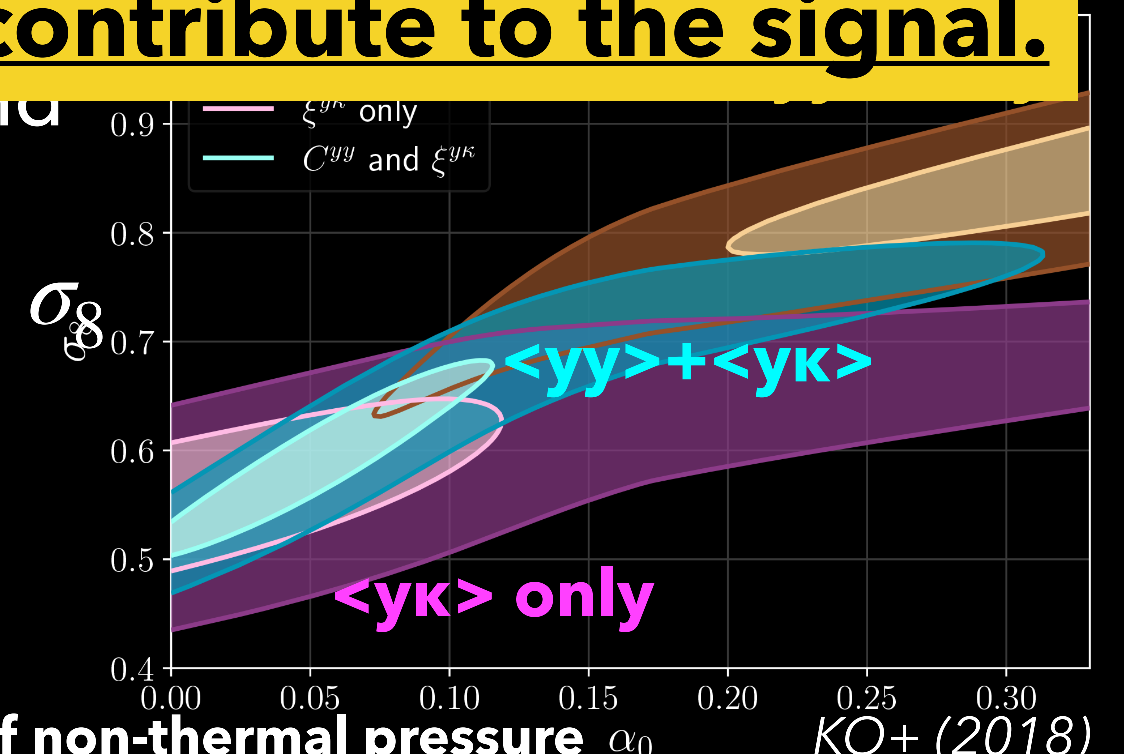

KO+ (2018)

Contents

1. Introduction

2. Method: model and covariance

3. Measurements and analysis of tSZ-WL cross-correlation with HSC and *Planck*

4. Future prospects and summary

Analytical Prediction of Signal

Theoretical prediction of cross spectra is based on ***halo model***.
All matter and gas is associated with halos.

$$C_\ell^{y\kappa} = C_\ell^{y\kappa(1\mathrm{h})} + C_\ell^{y\kappa(2\mathrm{h})}$$

$$C_\ell^{y\kappa(1\mathrm{h})} = \int dz \, \frac{d^2V}{dz d\Omega} \int dM \frac{dn}{dM} y_\ell(M,z) \kappa_\ell(M,z)$$

$$C_\ell^{y\kappa(2\mathrm{h})} = \int dz \, \frac{d^2V}{dz d\Omega} P_\mathrm{m}(k = \ell / D_A, z)$$

$$\times \int dM_1 dM_2 \frac{dn}{dM_1} b(M_1,z) y_\ell(M_1,z) \frac{dn}{dM_2} b(M_2,z) \kappa_\ell(M_2,z)$$

Correlation function can be obtained via Hankel transform.

$$\xi^{y\kappa}(\theta) = \int \frac{\ell d\ell}{2\pi} C_\ell^{y\kappa} J_0(\ell\theta)$$

Analytical Prediction of Signal

Theoretical prediction of cross spectra is based on ***halo model***.
All matter and gas is associated with halos.

$$C_\ell^{y\kappa} = C_\ell^{y\kappa(1\mathrm{h})} + C_\ell^{y\kappa(2\mathrm{h})}$$

well calibrated with *N*-body simulations

$$C_\ell^{y\kappa(1\mathrm{h})} = \int dz \, \frac{d^2V}{dz d\Omega} \int dM \frac{dn}{dM} y_\ell(M,z) \kappa_\ell(M,z)$$

$$C_\ell^{y\kappa(2\mathrm{h})} = \int dz \, \frac{d^2V}{dz d\Omega} P_\mathrm{m}(k=\ell/D_A, z)$$

$$\times \int dM_1 dM_2 \frac{dn}{dM_1} b(M_1,z) y_\ell(M_1,z) \frac{dn}{dM_2} b(M_2,z) \kappa_\ell(M_2,z)$$

Correlation function can be obtained via Hankel transform.

$$\xi^{y\kappa}(\theta) = \int \frac{\ell d\ell}{2\pi} C_\ell^{y\kappa} J_0(\ell\theta)$$

Analytical Prediction of Signal

Theoretical prediction of cross spectra is based on ***halo model***.
All matter and gas is associated with halos.

$$C_\ell^{y\kappa} = C_\ell^{y\kappa(1\mathrm{h})} + C_\ell^{y\kappa(2\mathrm{h})}$$

well calibrated with *N*-body simulations

Convergence Projection of NFW profile

$$C_\ell^{y\kappa(1\mathrm{h})} = \int dz \, \frac{d^2V}{dz d\Omega} \int dM \frac{dn}{dM} y_\ell(M,z) \kappa_\ell(M,z)$$

$$C_\ell^{y\kappa(2\mathrm{h})} = \int dz \, \frac{d^2V}{dz d\Omega} P_\mathrm{m}(k = \ell / D_\mathrm{A}, z)$$

$$\times \int dM_1 dM_2 \frac{dn}{dM_1} b(M_1, z) y_\ell(M_1, z) \frac{dn}{dM_2} b(M_2, z) \kappa_\ell(M_2, z)$$

Correlation function can be obtained via Hankel transform.

$$\xi^{y\kappa}(\theta) = \int \frac{\ell d\ell}{2\pi} C_\ell^{y\kappa} J_0(\ell\theta)$$

Analytical Prediction of Signal

Theoretical prediction of cross spectra is based on ***halo model***.
All matter and gas is associated with halos.

$$C_\ell^{y\kappa} = C_\ell^{y\kappa(1\mathrm{h})} + C_\ell^{y\kappa(2\mathrm{h})}$$

well calibrated with *N*-body simulations

$$C_\ell^{y\kappa(1\mathrm{h})} = \int dz \, \frac{d^2V}{dz d\Omega} \int dM \, \underline{\frac{dn}{dM}} \, \underline{y_\ell(M,z)} \, \underline{\kappa_\ell(M,z)}$$

Convergence Projection of NFW profile

$$C_\ell^{y\kappa(2\mathrm{h})} = \int dz \, \frac{d^2V}{dz d\Omega} P_\mathrm{m}(k = \ell / D_A, z)$$

$$\times \int dM_1 dM_2 \underline{\frac{dn}{dM_1}} \, \underline{b(M_1,z)} \, \underline{y_\ell(M_1,z)} \, \underline{\frac{dn}{dM_2}} \, \underline{b(M_2,z)} \, \underline{\kappa_\ell(M_2,z)}$$

Compton-y Projection of *pressure profile*

Correlation function can be obtained via Hankel transform.

$$\xi^{y\kappa}(\theta) = \int \frac{\ell d\ell}{2\pi} C_\ell^{y\kappa} J_0(\ell\theta)$$

Pressure Profile

✦**Universal pressure profile:** We can fit the pressure profile with X-ray or SZ observation. The GNFW profile (Nagai+, 2007) is used.

$$P_e(r) = P_{500}\left(\frac{M_{500}^{\mathrm{HSE}}}{3\times10^{14}\,h_{70}^{-1}\,\mathrm{M}_\odot}\right)^{0.12} \times \frac{P_0}{(c_{500}x)^{\gamma}[1+(c_{500}x)^{\alpha}]^{(\beta-\gamma)/\alpha}}$$

x = R/R_{500}

- The fitted pressure profile using **<u>62 nearby clusters</u>** observed by *Planck*.
- We rescale the mass and radius with hydrostatic bias:

$$M_{500}^{\mathrm{HSE}} = M_{500}(1-b_{\mathrm{HSE}})$$

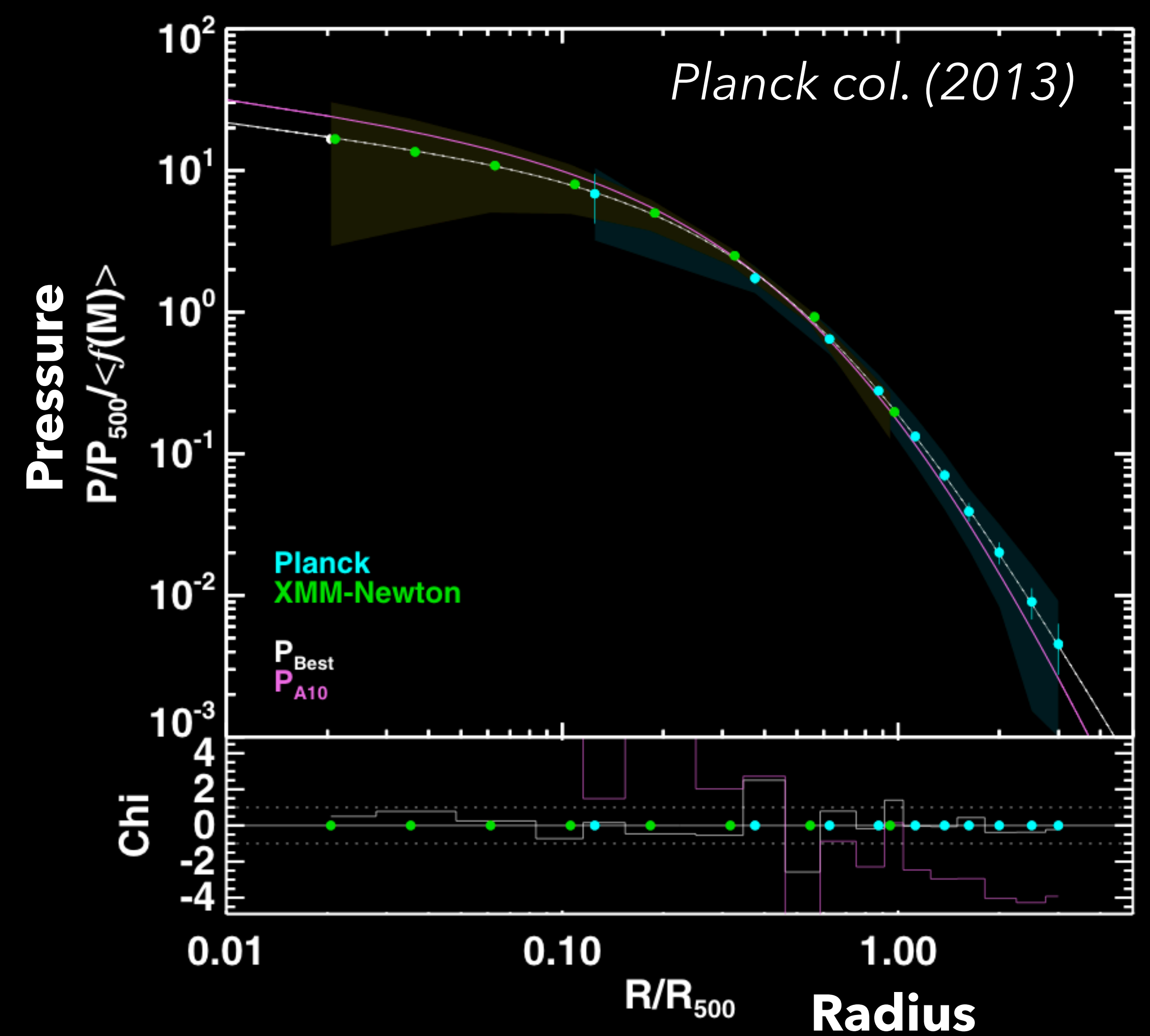

Mock WL and tSZ Maps

✦ ***All-sky simulations***

Takahashi+ (2017)
Shirasaki+ (2015)

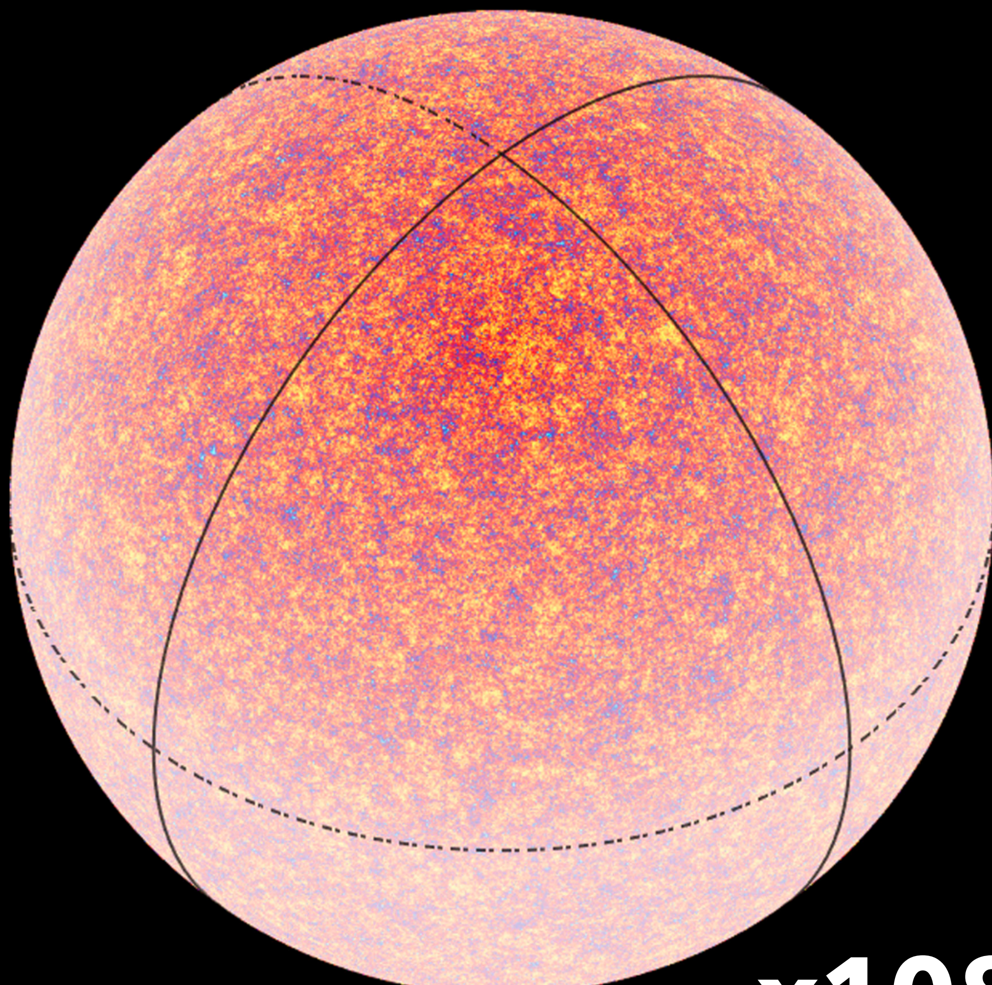

x108

✦The mock measurements are used to evaluate the covariance matrix.

WL **tSZ**

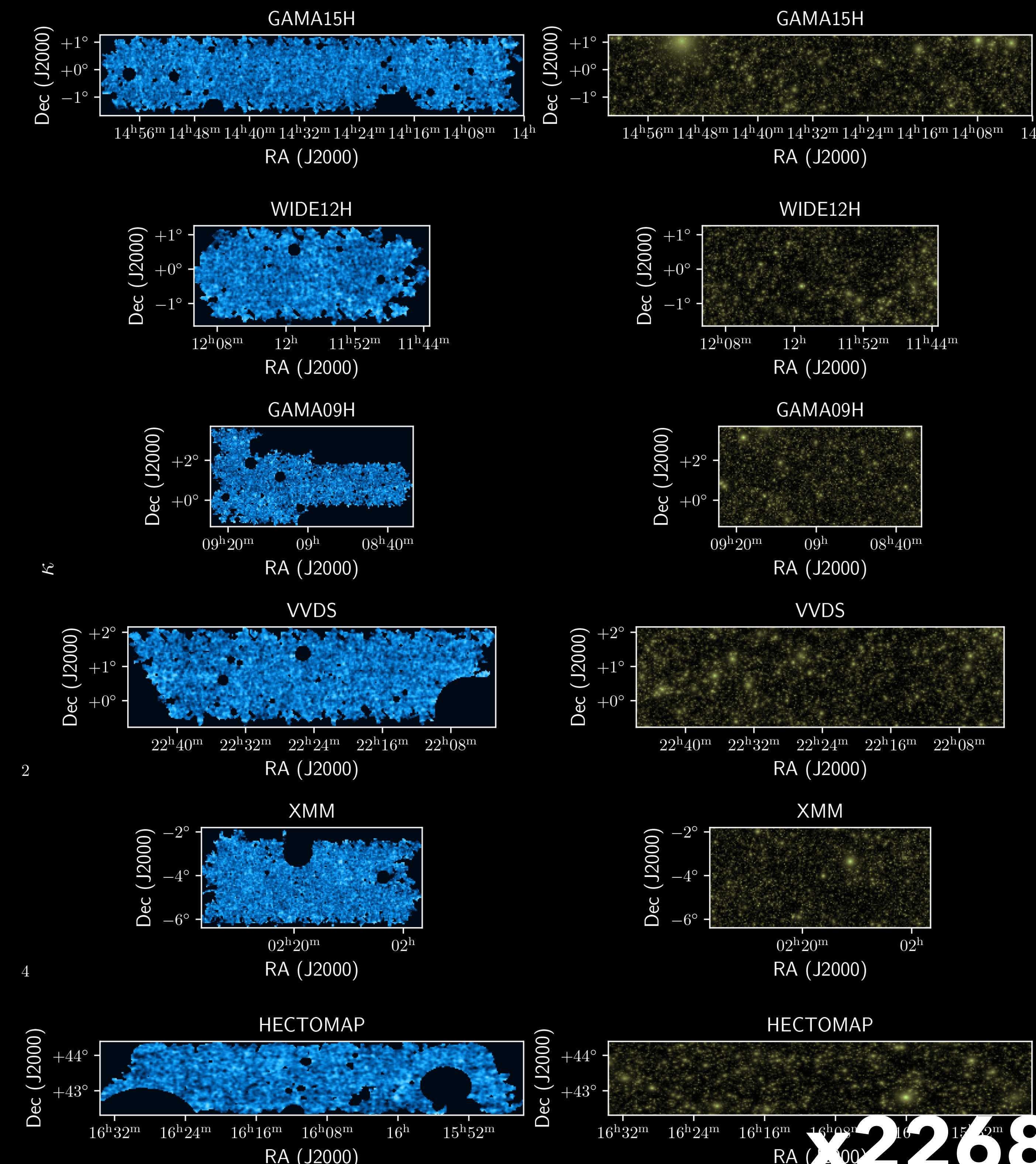

x2268

KO+ (2019)

Contents

1. Introduction

2. Method: model and covariance

3. Measurements and analysis of tSZ-WL cross-correlation with HSC and *Planck*

4. Future prospects and summary

Subaru Hyper Suprime-Cam

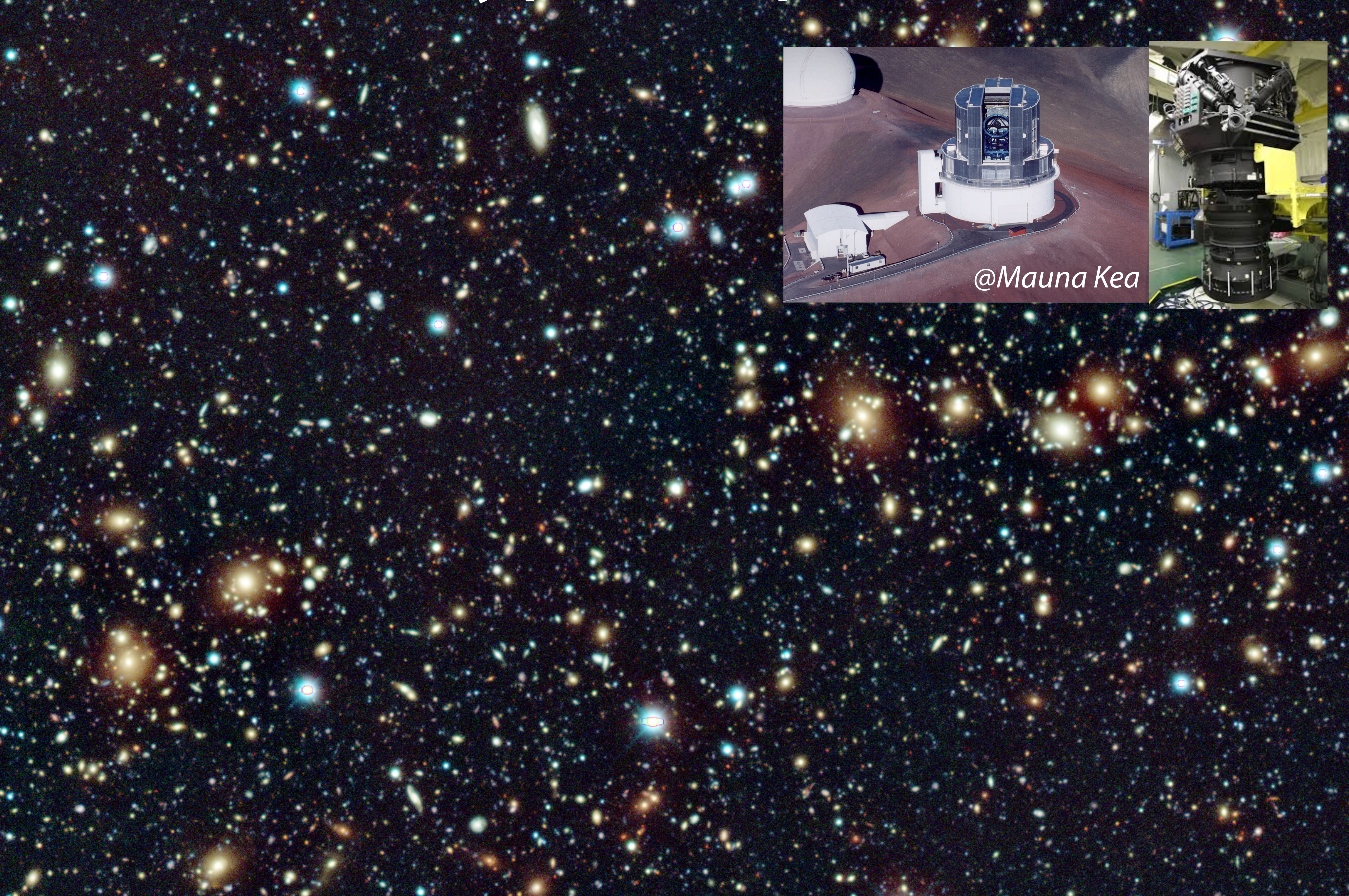

WL and tSZ Data

✦**HSC S16A**

Wide and deep WL survey (136.9 deg^2) with mean number density

$n_{\rm eff} = 24.6\,{\rm arcmin}^{-2}$ *cf. Mandelbaum+ (2017)*

✦***Planck* tSZ map**

constructed from 30 to 857 GHz data.

The sky coverage fraction is $f_{\rm sky} = 0.512$.

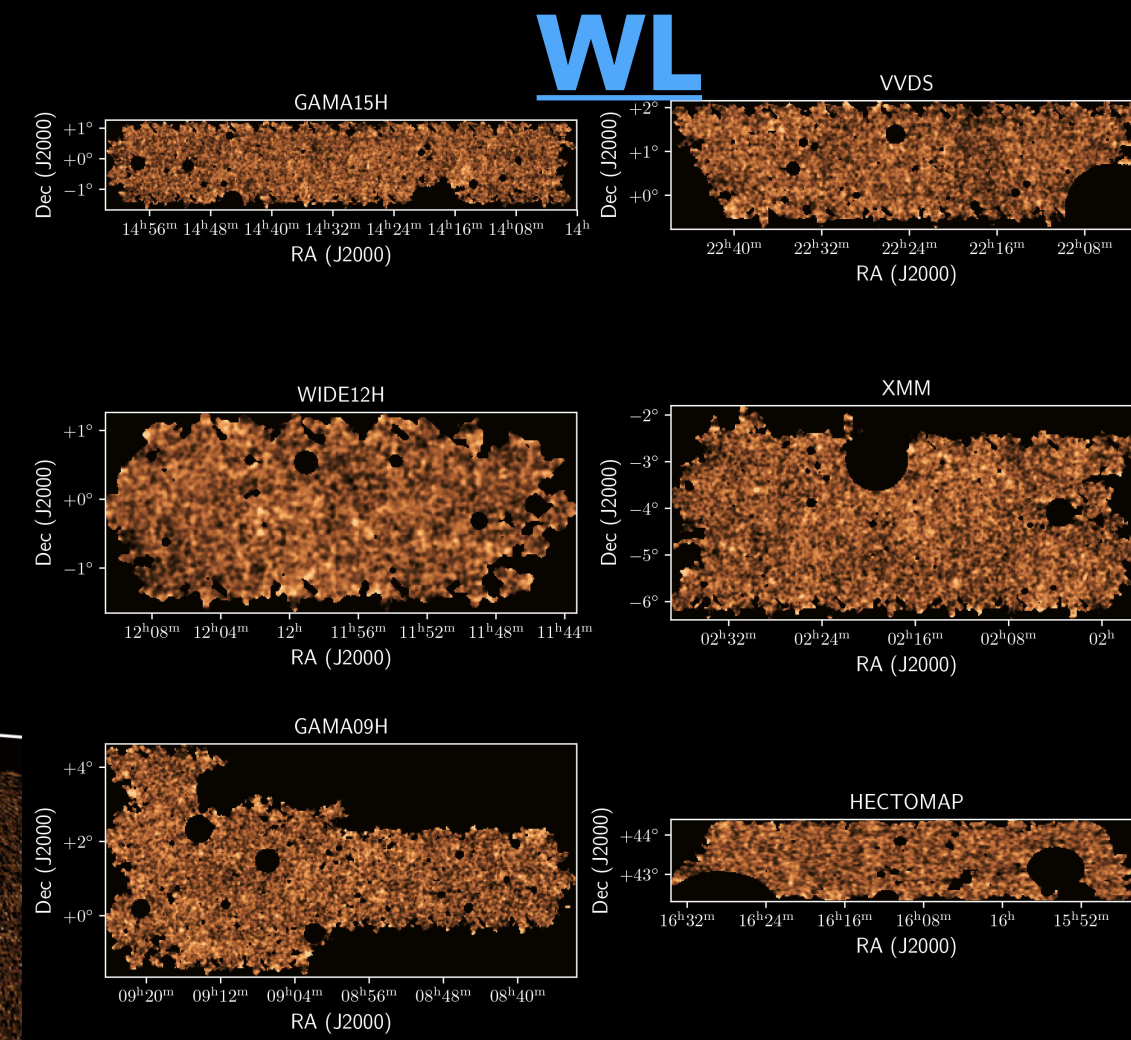

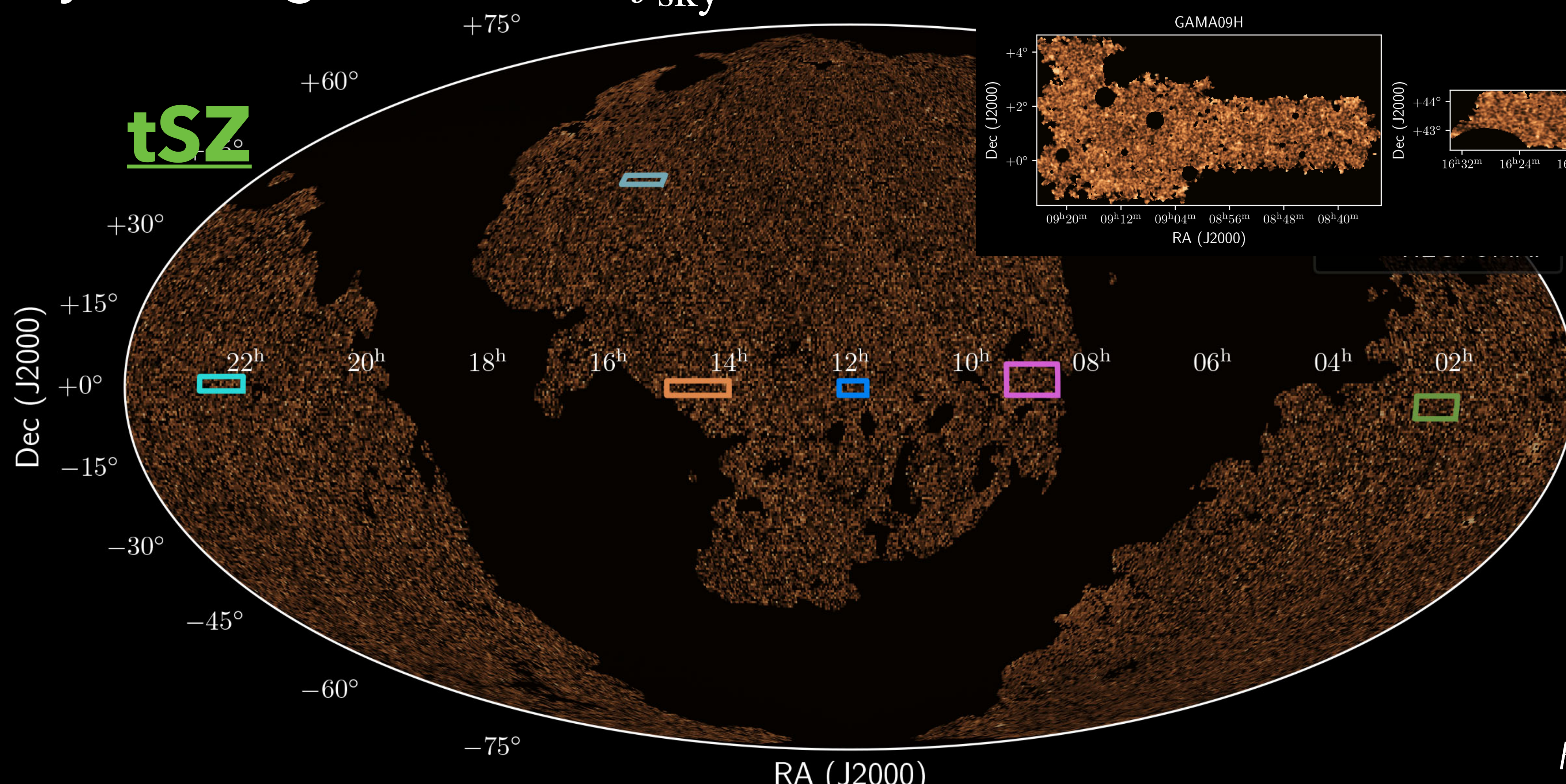

KO+ (2019)

Measurements of Cross-Correlation

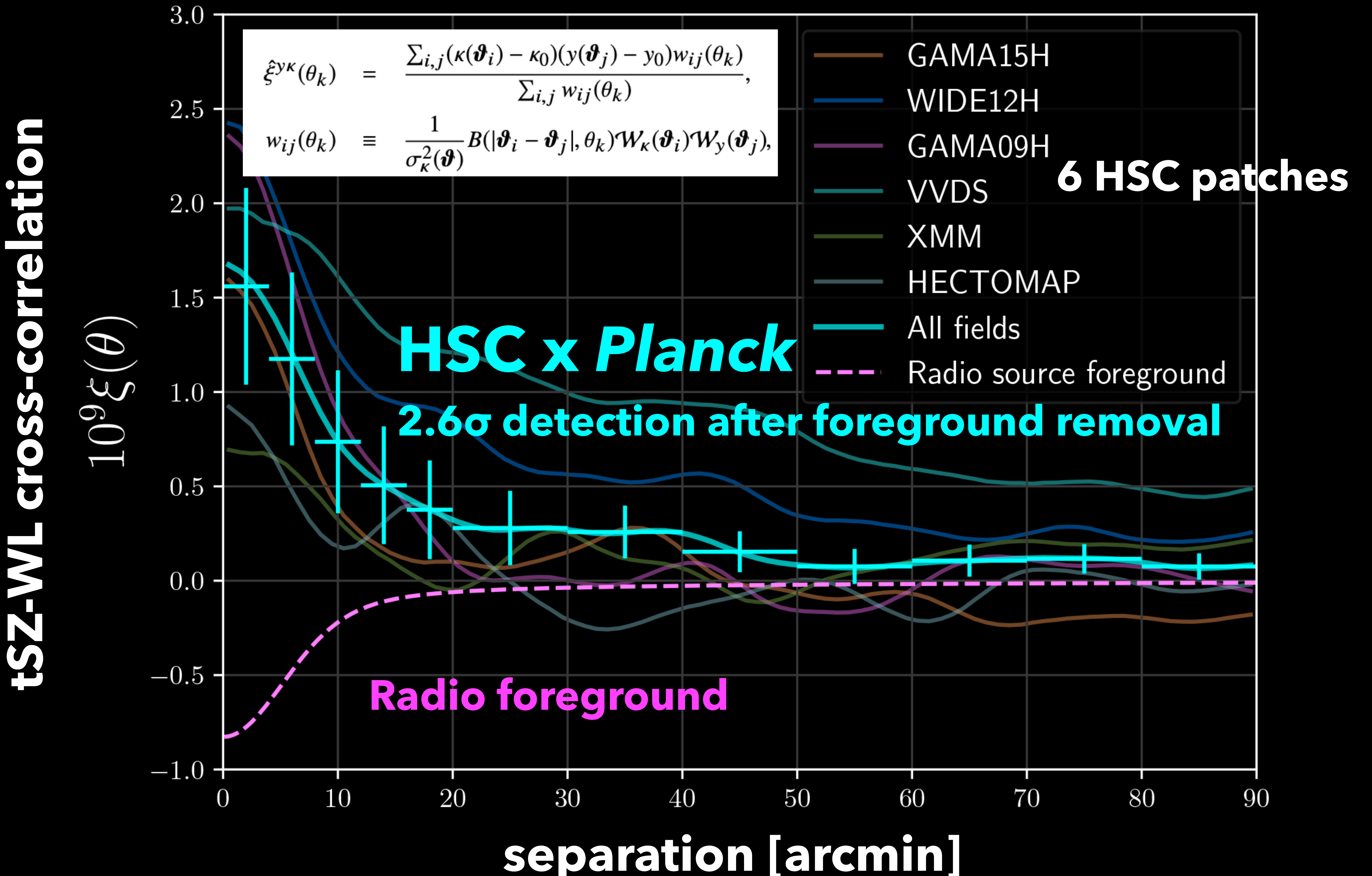

KO+ (2019)

Measurements of Cross-Correlation

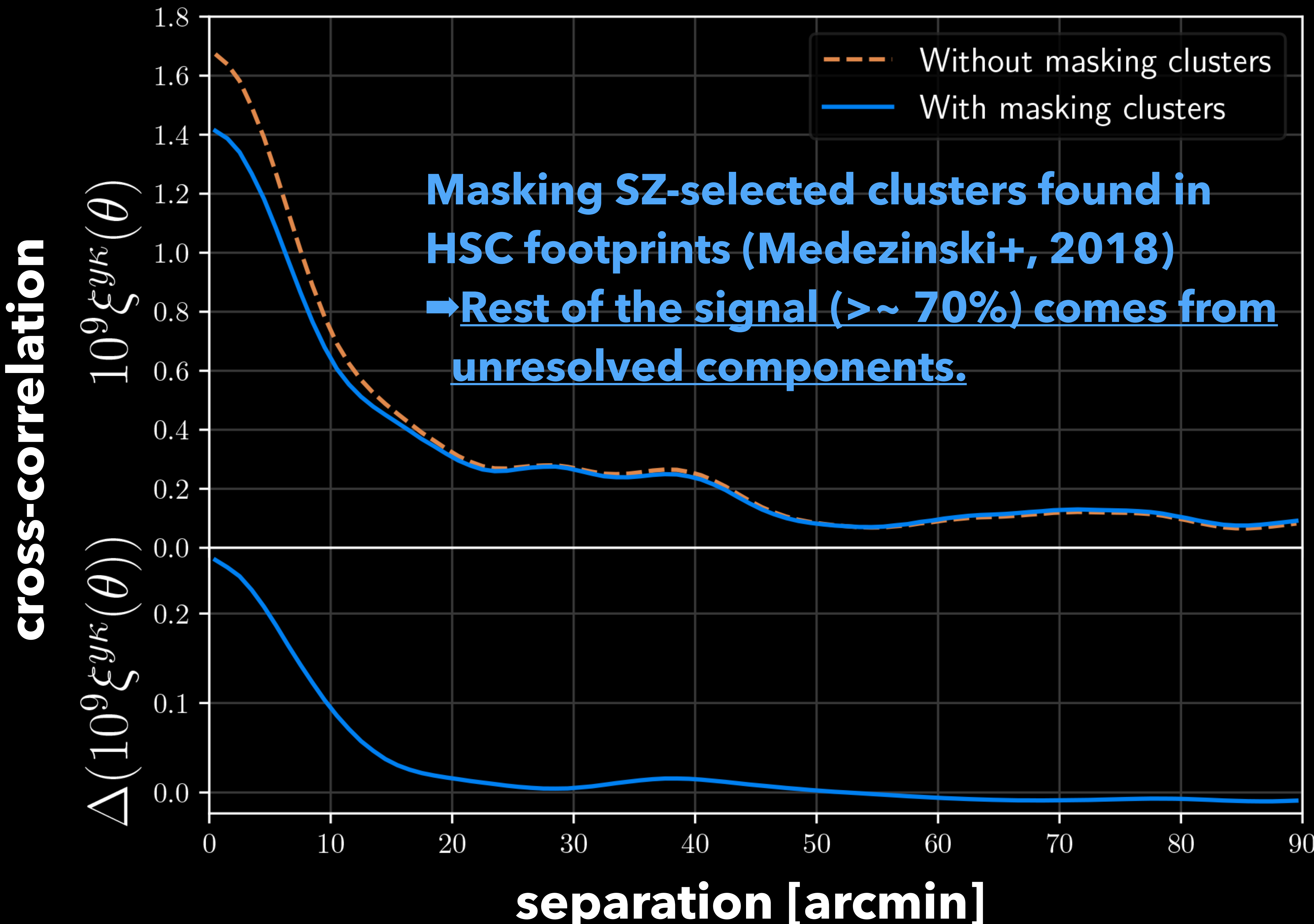

KO+ (2019)

Analysis

- **Data sets**
  1. tSZ auto-power spectrum only
  2. tSZ-WL cross-correlations only
  3. Joint of both

- **Foreground contamination**
  For tSZ auto-power spectrum *Bolliet+ (2018)*
  CIB, IR point sources, radio sources, and correlated noise
  For tSZ-WL cross-correlations *Shirasaki (2019)*
  Radio sources (flat-spectrum radio quasars, BL Lac)

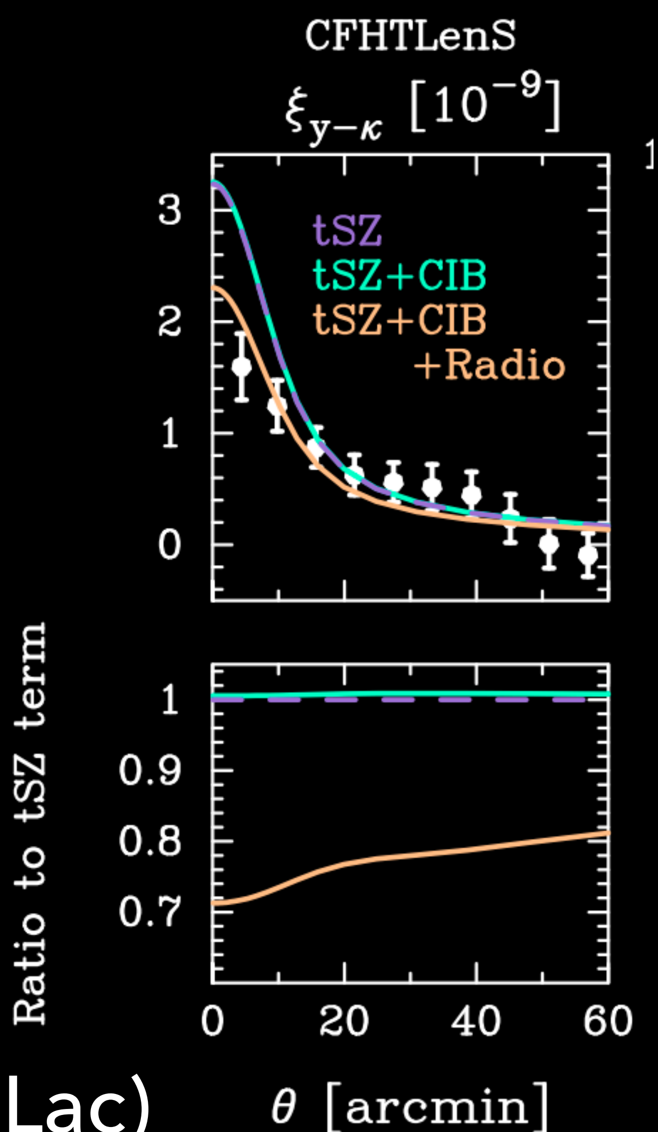

Shirasaki (2019)

- **Priors on cosmological parameters**
  1. combination of low-*z* LSS probes
  (HSC cosmic shear + JLA SN Ia + BOSS DR12 BAO/RSD)
  2. *Planck* 2018 TT,TE,EE+lowE+lensing

Constraints on Parameters

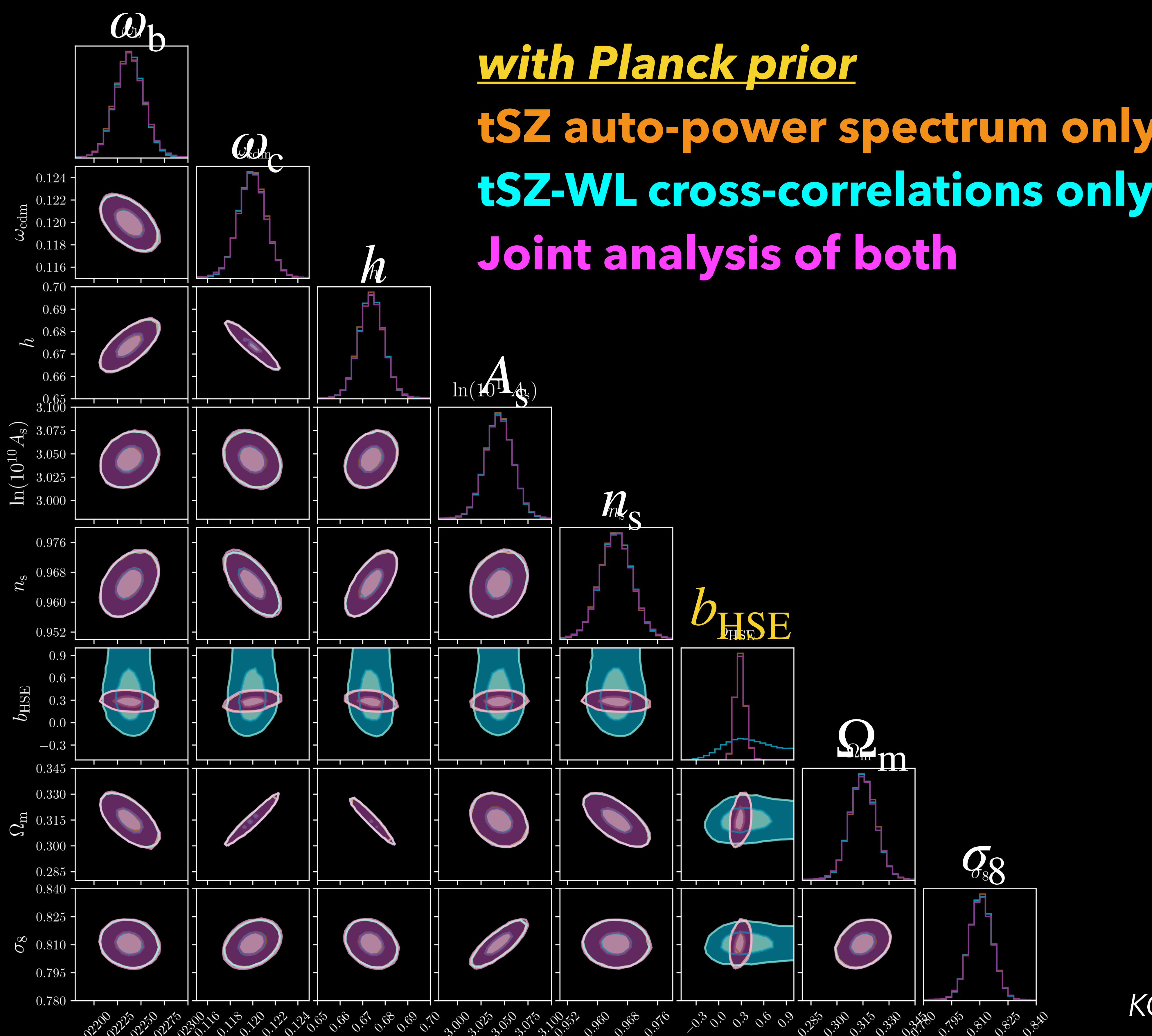

KO+ (2019)

Constraints on Amplitude and Mass Bias

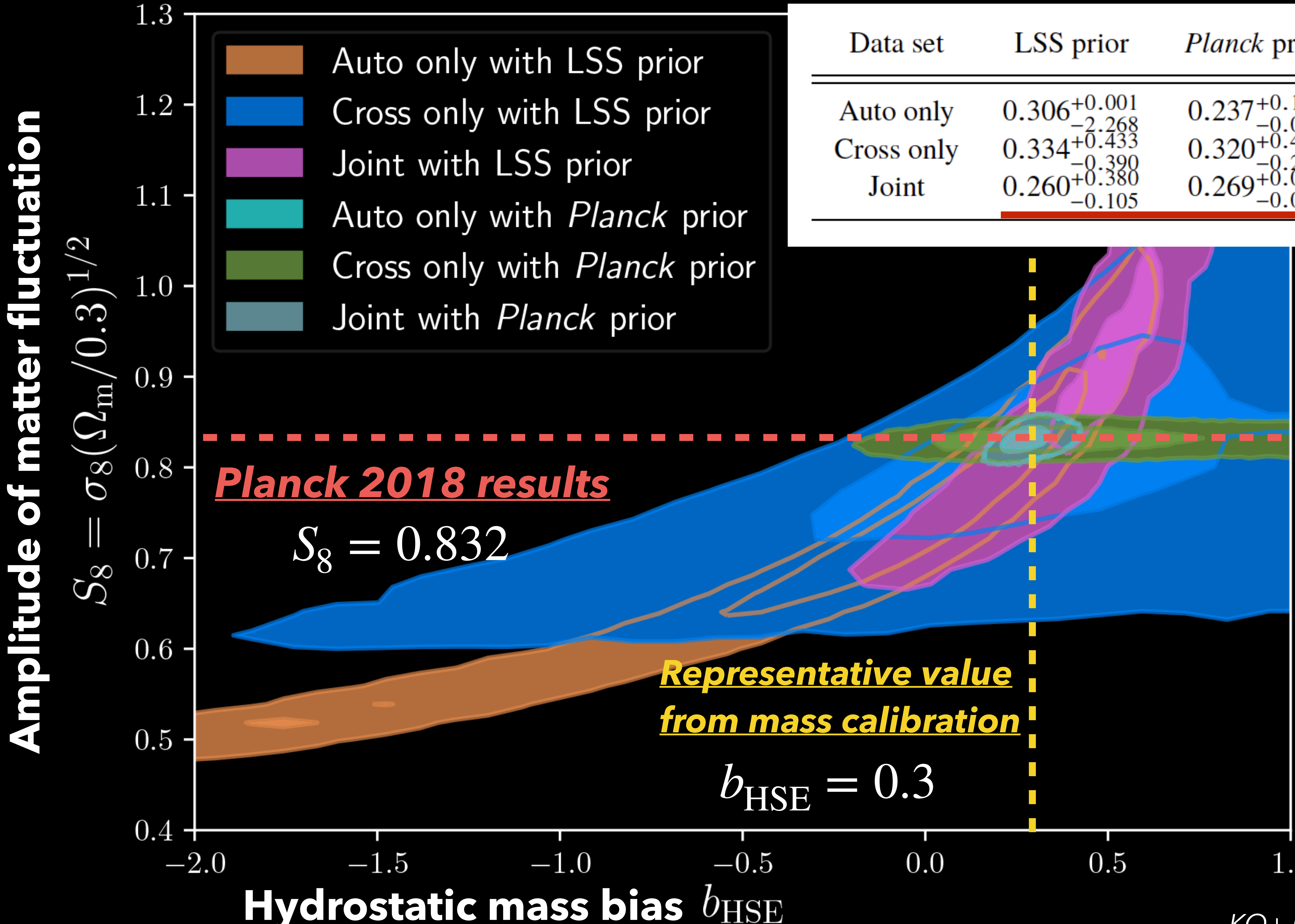

Data set	LSS prior	*Planck* prior
Auto only	$0.306^{+0.001}_{-2.268}$	$0.237^{+0.118}_{-0.010}$
Cross only	$0.334^{+0.433}_{-0.390}$	$0.320^{+0.437}_{-0.236}$
Joint	$0.260^{+0.380}_{-0.105}$	$0.269^{+0.089}_{-0.044}$

KO+ (2019)

Constraints on Amplitude and Mass Bias

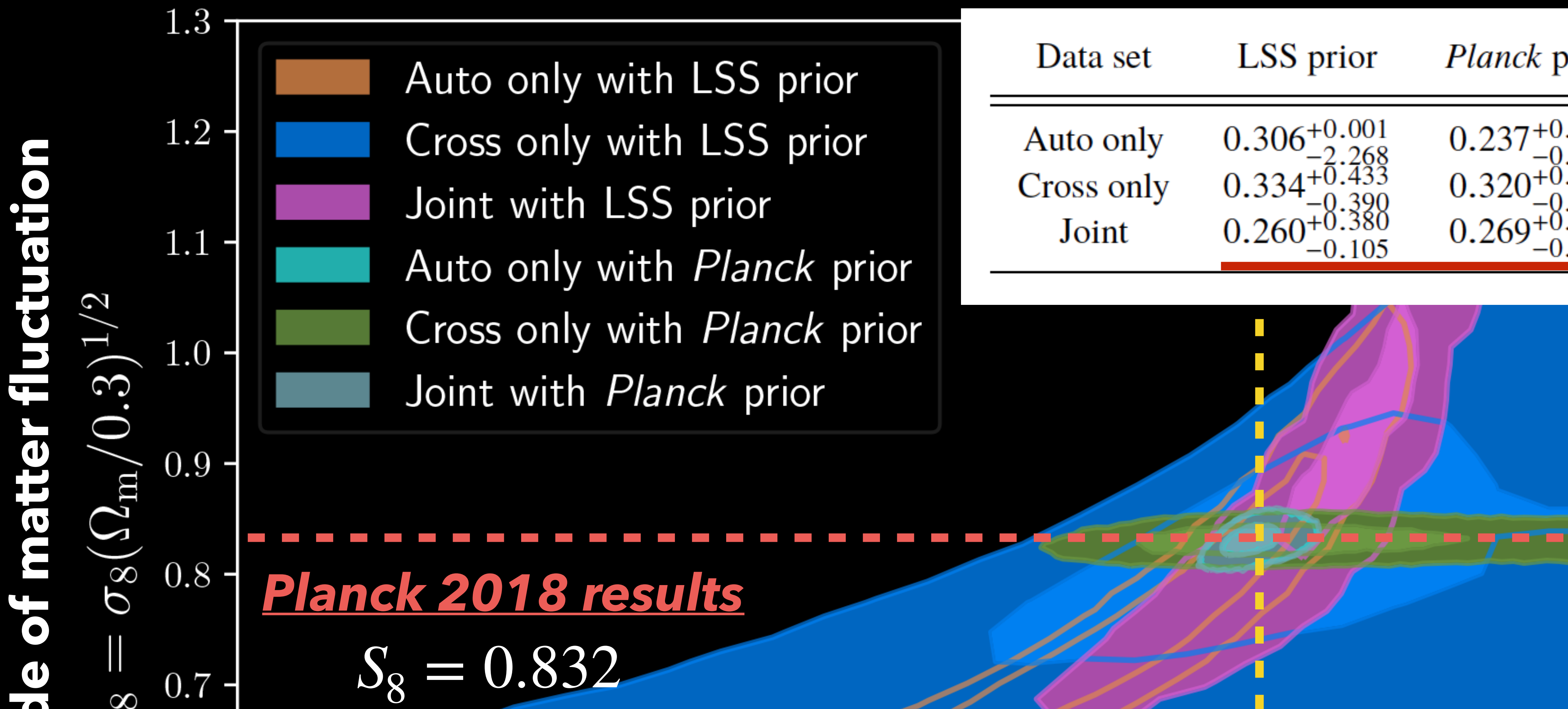

Data set	LSS prior	*Planck* prior
Auto only	$0.306^{+0.001}_{-2.268}$	$0.237^{+0.118}_{-0.010}$
Cross only	$0.334^{+0.433}_{-0.390}$	$0.320^{+0.437}_{-0.236}$
Joint	$0.260^{+0.380}_{-0.105}$	$0.269^{+0.089}_{-0.044}$

All of data sets give results consistent with each other and the inferred hydrostatic mass bias is ~0.3 though *low-mass or high redshift clusters* contribute to the appreciable fraction of tSZ auto-power spectrum and tSZ-WL cross-correlations.

Constraints on Mass Bias

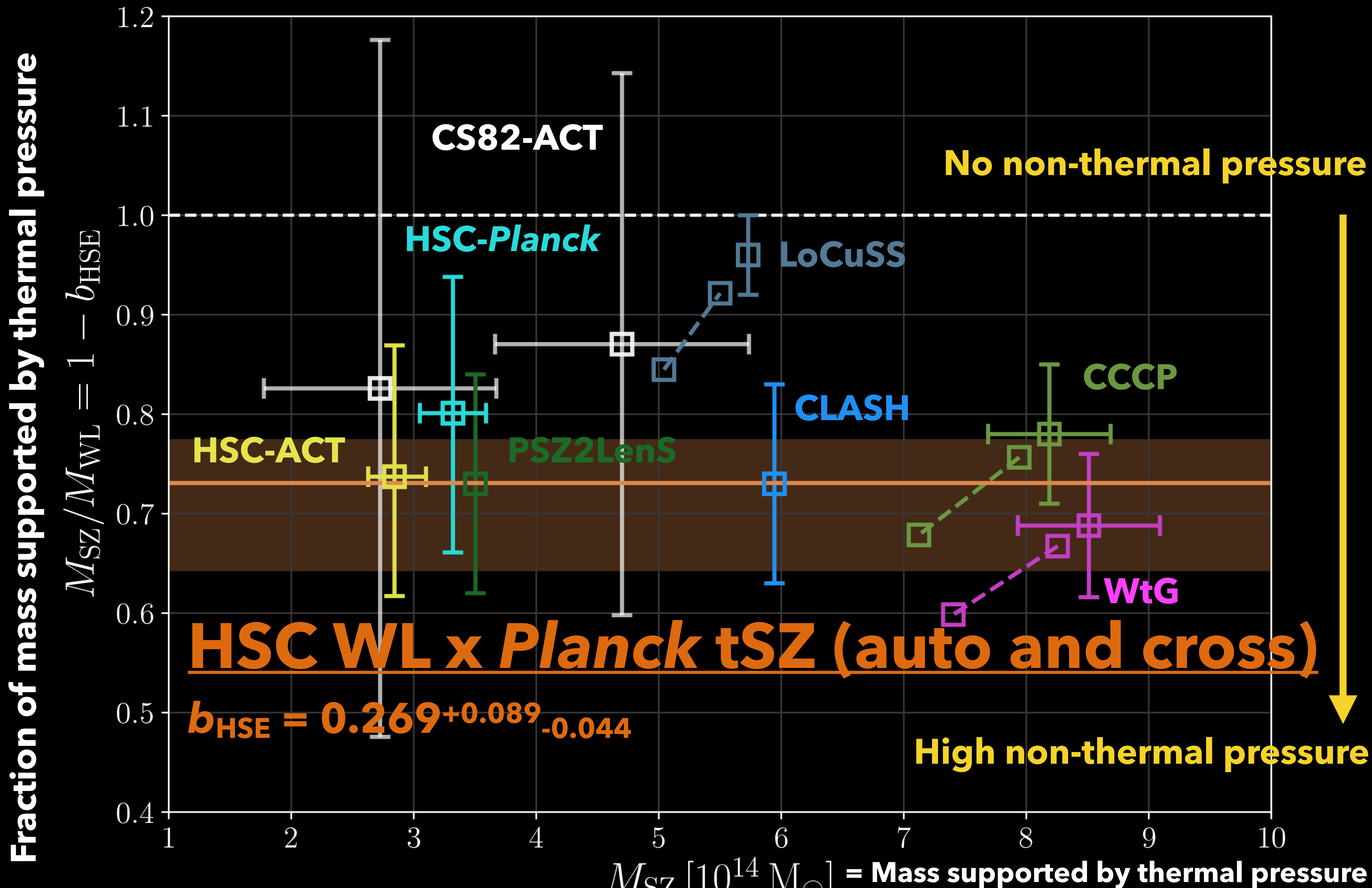

KO+ (2019)

Contents

1. Introduction

2. Method: model and covariance

3. Measurements and analysis of tSZ-WL cross-correlation with HSC and *Planck*

4. Future prospects and summary

Future Prospects

- **<u>Cross-correlations with HSC WL and ACT tSZ</u>**
  Atacama Cosmology Telescope (ACT) can measure the CMB temperature fluctuation with high resolution (beam size ~ 1 arcmin). By cross-correlating the data, we can probe into the fine structure of pressure profile.

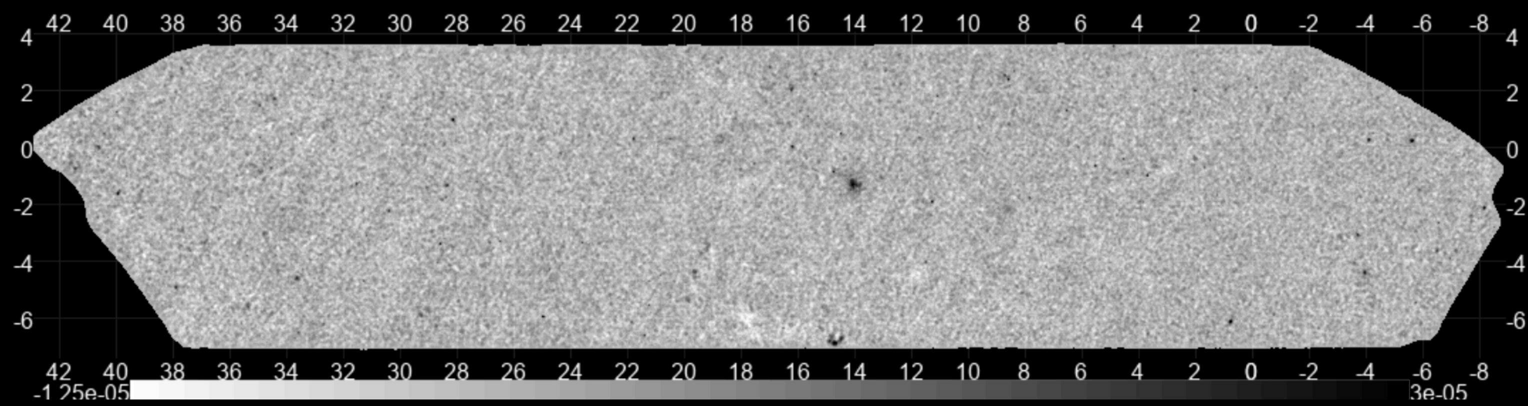

Madhavacheril+ (2019)

- **<u>Tomography technique</u>**
  Similarly to cosmic shear analysis, the whole galaxy samples can be divided according to its photo-z. Then, we measure cross-correlations for the subsamples.
  We can investigate the redshift evolution of hydrostatic bias.
  In this aspect, HSC has advantages of high source number density.

Summary

- Weak lensing and the thermal Sunyaev-Zel'dovich effect are promising probes into the large-scale structure and thermodynamical properties of intra-cluster medium.

- Cross-correlation is a powerful statistic with high S/N significance provides additional information useful for breaking degeneracy.

- Halo model calculation and *N*-body simulations are used to predict the signal and estimate the covariance matrix. This study presents the first attempt to estimate covariance matrix from realistic mock simulations.

- **HSC is the unique WL survey which can probe into the large-scale structures and cluster astrophysics at high redshifts, and the evolution of them by tomography.**